University of Minnesota
St. Anthony Falls Hydraulic Laboratory

Project Report No. 188

PART I

FLOW AROUND CIRCULAR CYLINDERS:

UNSTEADY LOADS

Prepared by

César Farell

Prepared for

NATIONAL SCIENCE FOUNDATION
Washington, D. C.

November, 1979
Minneapolis, Minnesota

TABLE OF CONTENTS

ABSTRACT

A state-of-the-art review of the problem of determination of the fluctuating loads on rigid circular-cylindrical structures in uniform flows with and "without" free stream turbulence is presented. Particular attention is paid to the effects of surface roughness of the structure and of Reynolds number, and to the definition and characterization of the various flow regimes, subcritical, critical, supercritical, and transcritical. Flow three-dimensionality and length-to-diameter, wall interference, and model-end-condition effects are also discussed. Problems requiring additional research are identified.

LIST OF FIGURES

Figure 5(a)

Strouhal numbers after reappearance of organized shedding. Smooth cylinders: ▽ , Roshko (61); Jones et al (41) (results in region of definite vortex shedding): ▼ , M = 0.3; ◇ , M = 0.2. Roughened cylinders: Nakamura (54): o , dist. roughness, k/d = 2.5×10^{-3}; ◪ , dist. roughness, k/d = 8.5×10^{-3}; ⌀ , roughness strips; ◩ , Tani (76).

Figure 5(b)

Strouhal numbers after reappearance of organized shedding. Data of Szechenyi (74): x , smooth cylinder; □ , k/d = 1.5×10^{-4}; ■ , k/d = 2.5×10^{-4}; o , k/d = 5×10^{-4}; ● , k/d = 7.5×10^{-4}; △ , k/d = 10^{-3}; ▲ , k/d = 1.75×10^{-3}.

PART I

FLOW AROUND CIRCULAR CYLINDERS: UNSTEADY LOADS

INTRODUCTION

While considerable progress has been made in the analysis of the mean wind loading on circular cylinders and other rounded structures like chimneys and cooling towers, specifically with regard to surface roughness effects and to flows at high Reynolds numbers (see e.g. (1)*, (28), (57), (59)), investigations of the unsteady components of the wind loading on such structures are still needed, in particular with regard to the two aforementioned problems and to free stream turbulence effects. On cooling towers, specifically, tensile wind stresses and compressive dead load stresses are of comparable magnitude and hence their difference is quite sensitive to small changes in wind loading; information on the dynamic wind stresses (which may be of the same order of magnitude as the static stresses) is therefore needed for design purposes and the problem has been the object of recent attention (see e.g. (5), (6), (36), (59)). The considerable reductions in the r.m.s. values of the pressure fluctuations in the presence of surface roughness that have been reported (8), (18), (59), (73) but not fully interpreted due to the difficulty of obtaining comprehensive data highlight the need for a better understanding of the flow phenomena.

More generally, knowledge of the details of the pressure fluctuations occurring on the surface of a solid boundary interacting with a complicated flow field is of considerable importance in a variety of practical problems. Many problems in the area of aerodynamic sound can be associated with the interaction of the unsteady flow structure in the vicinity of the body surface with the body itself. The sound radiated by solid surfaces in the presence of unsteady flows (see e.g. (29)) can be partly represented by a dipole distribution whose strength depends upon the characteristics of the surface-pressure fluctuations, the contribution from the dipoles being dominant in many cases. Sound transmission through a boundary surface depends essentially upon the characteristics of the pressure fluctuations acting on

---

*Numbers in parenthesis indicate references beginning on page 40.

it, as does also of course the load on any structure interacting with a fluid flow, particular cases being the cooling tower design problem mentioned in the preceding paragraph, the wind loads on other circular cylindrical objects like smoke stacks, silos, and rocket launchers, and the loads on cylindrical elements of sea structures.

The problems described are rather complex and not amenable to direct analytical treatment. Decomposition into simpler problems is necessary, in the hope that if the simpler problems can be solved, an appropriate combination of the solutions may reveal in at least an approximate manner the general behavior of the solution of the initial problem. Even after such a decomposition is made, one is still faced in the present case with complex phenomena, including separation and transition to turbulence, and experimental investigations are needed to guide the theory and to understand the flow. This review will focus mainly on investigations of fluctuating loads on rigid circular cylinders in uniform streams, particular attention being given to the effects of free stream turbulence and surface roughness. The effects of a velocity gradient in the oncoming flow are not discussed here in the interest of conciseness, and to permit focusing on the important effects of various turbulence characteristics. Earlier related reviews can be found in (14), (38), (47), (49), (52), (63), and (67).

GENERAL CONSIDERATIONS

Independent variables for the problem just described are the Reynolds number, $Re = Ud/\nu$ (U = velocity of uniform stream, d = cylinder diameter, or mean diameter of the structure, and ν = kinematic viscosity of the fluid), the pertinent geometric parameters (for a circular cylinder spanning a cross section, the cylinder length-to-diameter ratio, ℓ/d, and the blockage ratio, d/b, where b = test section width), the free stream turbulence characteristics (one needs at least a relative turbulence intensity, $T_u = u/U$, where $u = \sqrt{\overline{u'^2}}$ and u' = longitudinal velocity fluctuation, and a relative turbulence length scale, L_x^u/d or L_y^u/d where L_x^u and L_y^u are respectively the longitudinal and lateral length scales of the u' fluctuation), and adequate parameters describing the surface roughness of the structure (at least a roughness height, k, or preferably an equivalent roughness height, k_s; see (26) for a discussion of this problem). The functional relationships

between these parameters and the dependent parameters that characterize the loading on the structure exhibit drastic changes with Re. Four flow regimes, each characterized by a special boundary layer behavior, can be identified (but see a critique of the following definitions below): subcritical (purely laminar separation); critical (laminar separation followed by reattachment and delayed final flow separation); supercritical (transition occurring ahead of separation and moving upstream); and transcritical (transition located sufficiently close to the forward stagnation line so that the flow becomes independent of Re). The terminology (and the definitions themselves) vary among various authors, and the boundaries between the various flow regimes may not be sharply defined, depending in particular on the parameter considered.

For conciseness, important features of several investigations are summarized in Table 1, without attempting to be exhaustive. (Additional relevant references are given in the text and in the bibliography.) Fung (30), Jones et al (41), and Richter and Naudascher (60) measured lift and drag forces over finite cylinder lengths using force-balance methods; in other investigations lift and drag were obtained through analysis of the simultaneous pressure signals at sufficient points at instrumented sections of the cylinder. Jones et al (41) and Szechenyi (73) used pressurized wind tunnels with side wall slots or perforations to correct for blockage effects, while Richter and Naudascher (60) and Warschauer and Leene (81) used high-pressure water tunnels; closed-section wind tunnels were used in the other investigations, with the exception of some of Korotkin's (44) experiments which were carried out in an open section tunnel. Schmidt's (69, 70) model was a cantilevered cylinder with a blunt end; one of the cylinders ($\ell/d = 6.9$) investigated by Warschauer and Leene was also cantilevered. Fung's (30) cylinder model had unsealed, 0.02 in. wide and 0.9 in. deep slots between the instrumented and outer cylinder sections (which had a significant effect on the flow in the wake according to Fung).

TABLE 1: IMPORTANT FEATURES ON SEVERAL INVESTIGATIONS

Reference	Measurements	Re_{-6} x10	Regime Sub.	Cri.	Sup.	d/b	ℓ/d	k/d x10^{3}	T_u(%)	L^u_x/d
Fung (1960)	Lift and drag spectra	0.3-1.4		x		.105	5.69	"s"*		
Humphreys (1960)	Lift and drag fluctuations; flow visualization	0.04 0.6	x	x		0.152	6.56	"s"	1.0	
Roshko (1961)	Velocity fluctuation spectra; mean pressures	1.5 9	x	x	x	0.136	5.67	0.011		
Tani (1964)	Velocity flucuation spectra; flow visualization; trip wires	0.03-1.0	x	x	x	0.07 0.164 0.317	14.3 6.10 3.15	"s" 0.9×10^{-3} 2.3×10^{-3}		
Schmidt (1965)	Lift and drag cross correlations and cross spectra	0.38-0.75		x		.071	8.10	"s"		
Jones et al (1969)	Lift spectra	0.36		x	x	.187	5.34	0.002	0.2	
Bearman (1969)	Velocity fluctuation spectra; mean pressures	0.10-0.75	x	x		.065	12.0	"s"	0.2	
Warschauer and Leene (1971)	Correlations and spectra of pressure flucuations	0.3-3.9	x	x	x	0.058 0.118 0.118 0.198	17.2 8.5 6.9 5.0	0.007 0.003 0.003 0.002	0.1	
van Nunen et al (1971)	Pressure and lift and drag spectra	0.5-7.7	x	x	x	0.167?	6 ?	"s"		

*"s": Nominally smooth cylinder (k/d not known)

TABLE 1: IMPORTANT FEATURES ON SEVERAL INVESTIGATIONS

(Continued)

Reference	Measurements	Re_{-6} x10	Regime Sub.	Cri.	Sup.	d/b	ℓ/d	k/d x10^3	T_u (%)	L^u_x/d
Surry (1972)	Pressure, drag and lift cross correlations and cross spectra; turbulent streams	0.034-0.044	x			.028	60	"s"	2.5 10.5 10.0 14.7	9.80 0.36 4.30 4.40
Batham (1973)	Pressure correlations and spectra; smooth and rough models; turbulent streams	0.111 0.235	x	x	x	.050	6.65	"s" 2.17	0.5 12.9	 0.50
Bruun and Davies (1975)	Pressure and velocity fluctuation spectra and correlations; turbulent streams	0.08-0.48	x	x		.131	9.82	"s"	.16 .17 10.5 11.0 3.8	 0.55 0.19 0.35
Szechenyi (1975)	Lift spectra; smooth and rough models	0.096-4.2	x	x	x	.077 .128 .179 .230	9.33 5.60 4.0 4.38	"s" 0.15-2.00	4.0 0.3	
Korotkin (1976)	Mean pressures; visualization	0.067-1.67	x	x		open section	5.0 25.0	"s"	0.5	
		0.6		x		0.12	8.3	"s"	0.03	
Richter and Naudascher (1976)	Lift and drag spectra	0.02-0.04	x	x		.167 .250 .333 .500	8.60	0.8	0.5	
Sonneville (1976)	Velocity, pressure and lift and drag cross correlation and cross spectra	0.01-0.065	x			.056	12.9	"s"	0.3	

CYLINDERS IN LOW-TURBULENCE STREAMS

A. Three-dimensional and Other Effects

The physical changes that take place in the flow as Re increases are reflected in particular in the value of the drag coefficient, C_d, which drops sharply as the laminar separation-turbulent reattachment bubble appears (but see discussion below) and then increases and attains a constant value at large Re. Corresponding transitional changes are exhibited by other flow parameters, as depicted in Fig. 1, where selected curves representing measurements by various authors are presented to indicate the general trends. A discussion of the functional dependence of C_d and other mean-pressure-distribution parameters (base and minimum pressure coefficients, C_{pb} and C_{pm}, pressure rise to separation, $C_{pb} - C_{pm}$, separation angle, ϕ_S, and angle of transition, ϕ_T) on Re and surface roughness is given in (34), (28), and (35) and specifically for cooling towers in (26). It is shown in these references that the drag coefficient, C_d, while strongly dependent on relative roughness (in particular in the range of large Re, where Reynolds number independence obtains) is also rather sensitive to factors such as length-to-diameter ratio, tunnel blockage, end conditions of the model, and side wall conditions of the tunnel. In particular, it is suggested that the marked differences in the C_d data from various sources for smooth cylinders at large Re (see Fig. 2 reproduced from (34)) may be due to a large extent to wall interference effects associated with the use of slotted-wall tunnels to compensate for blockage. Such differences are not present in the data from the same sources for the pressure rise to separation, $C_{pb} - C_{pm}$ (see Fig. 3 reproduced from the same source), a quantity closely related to boundary layer characteristics and relatively insensitive to blockage and end conditions effects (25, 26) and strongly dependent on relative roughness, in particular in the Re independent range.

While the pressure rise to separation thus affords a basis, albeit limited, for comparison of circular cylinder data (and also cooling-tower and other rounded-structure data) obtained under different experimental conditions, for meaningful evaluation of other mean flow data and, particularly, of flow fluctuation data, there is still the difficulty of taking into account all the parameters that might have an effect on the flow. The vortex shedding phenomenon is extremely sensitive to three-dimensional

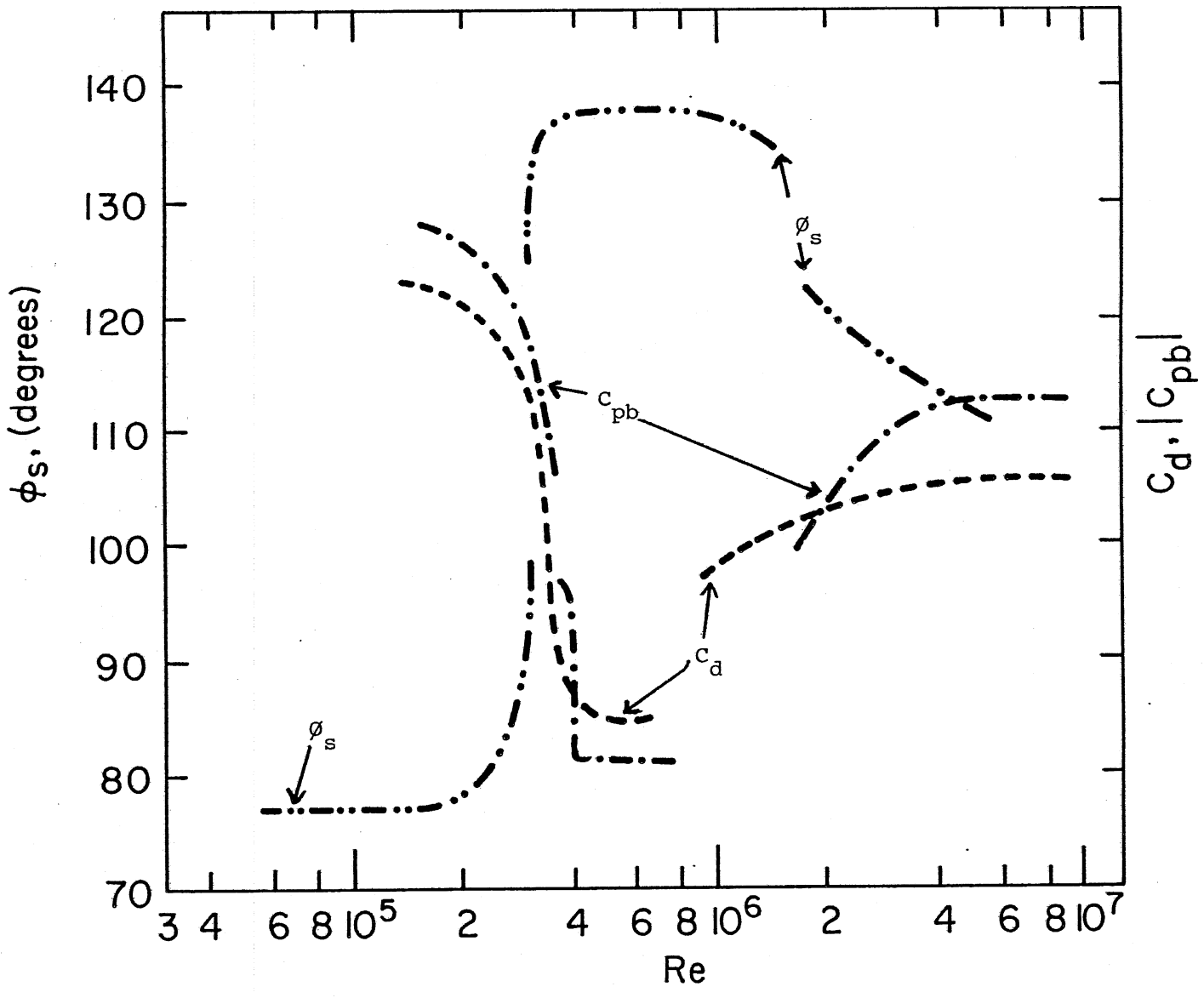

Fig. 1(a) - Variation of mean quantities with Reynolds number. (Only mean curves are drawn for illustration .) -·-· : ϕ_s , Achenbach(4); -·- : C_{pb} , Bearman (11), Roshko (61); – – – : C_d , Güven et al (34), Achenbach (4), Roshko (61).

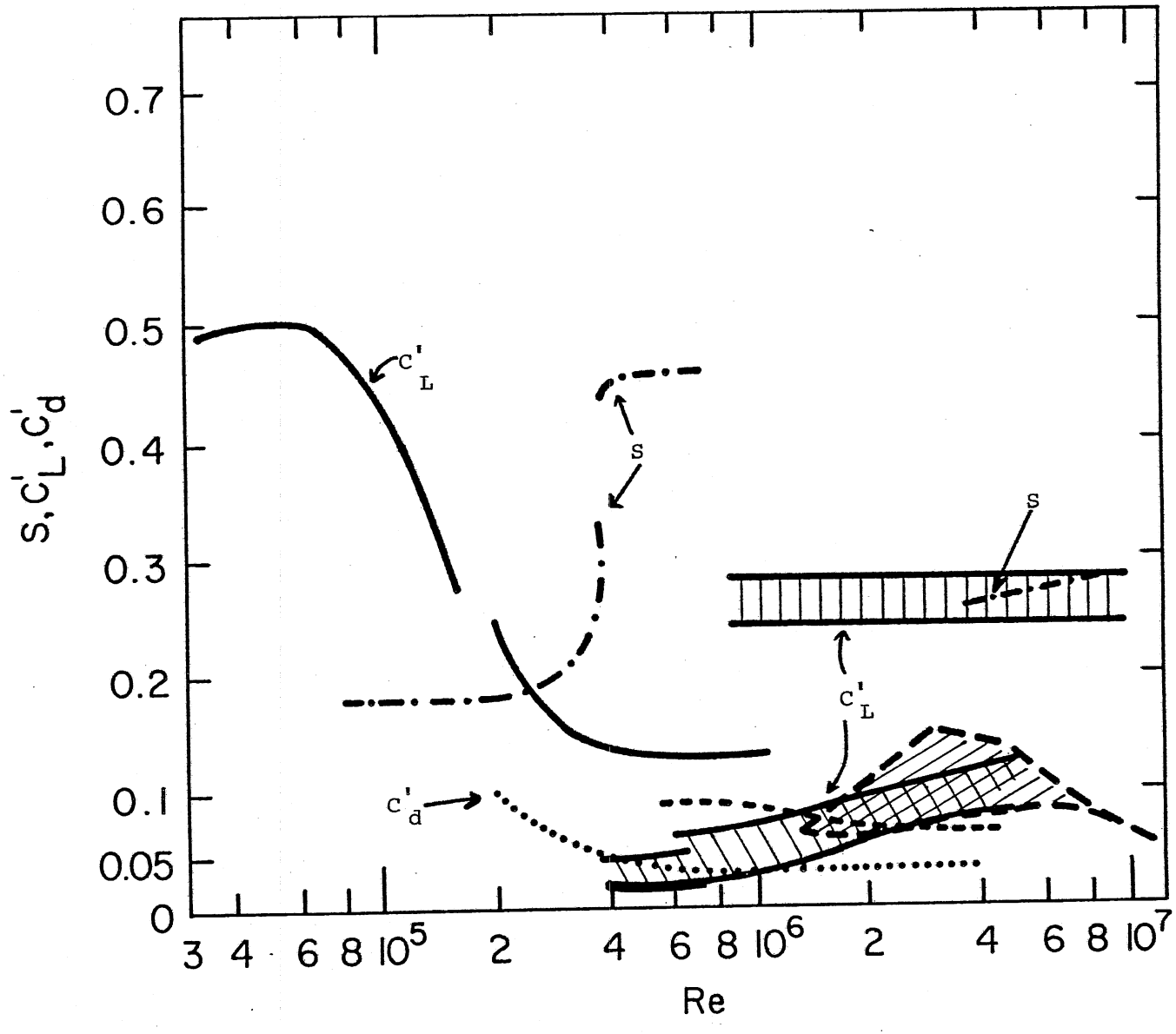

Fig. 1(b) - Variation of mean quantities with Reynolds number. (Only representative mean curves are drawn for illustration of trends.) ———: C'_L, Sonneville (71), Humphreys (37), Fung (30); – – – – – – : C'_L, Szechenzi (74), smooth cylinder; ||||||| : C'_L, Szechenzi (74), distributed roughness (envelope of asymptotic values for large Re shown only); \\\\\\ : C'_L, Schmidt (69, 70); /////// : C'_L, Jones et al (41); ..... : C'_d, Fung (30), Schmidt (69), van Nunen et al (58); -·-·-·- : S, Bearman (11), Roshko (61).

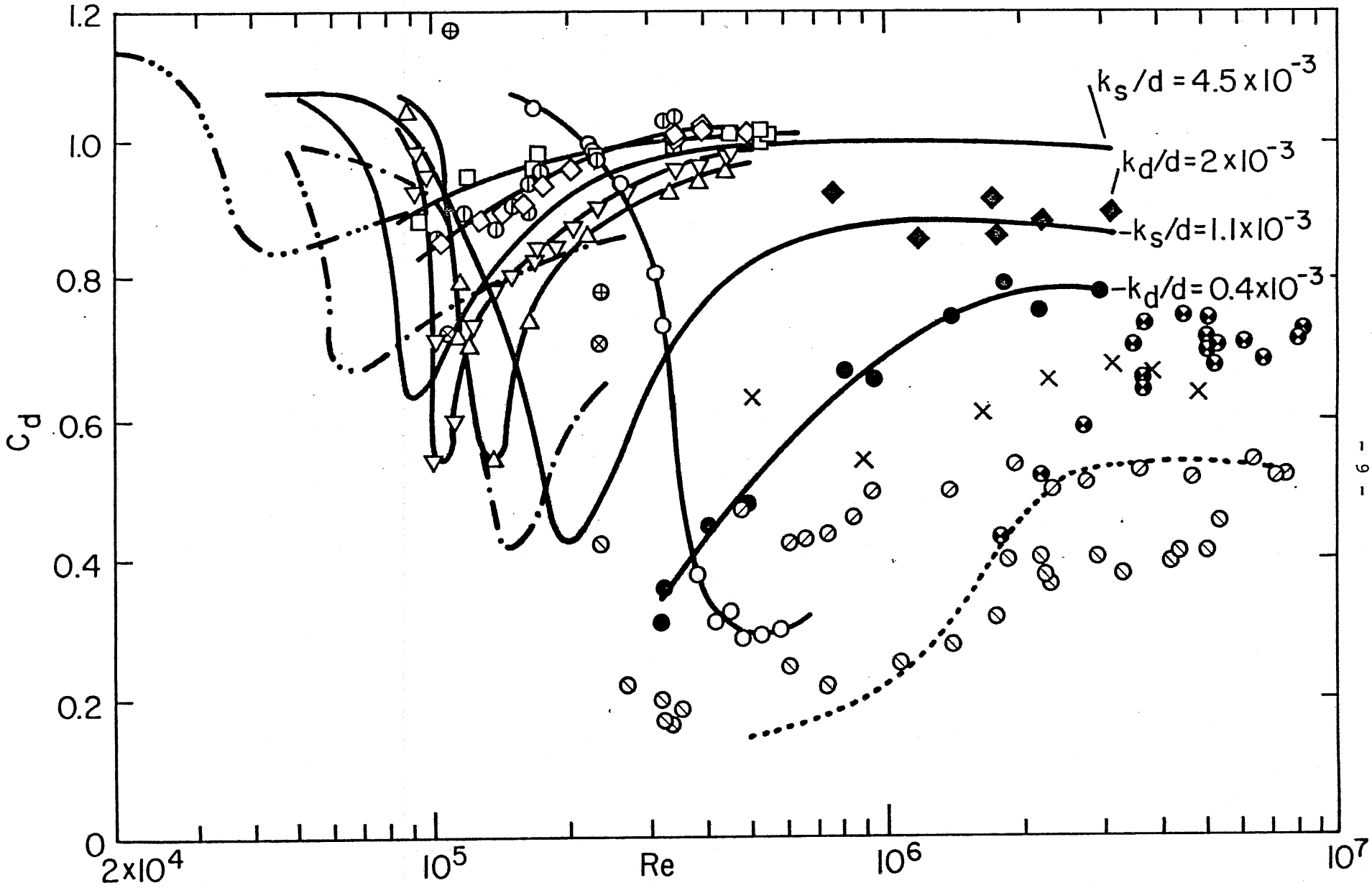

Fig. 2 - Drag coefficient of cylinders with distributed roughness. ———, Achenbach (1971). Fage and Warsap (1929): -·-, $k_s/d = 2\times10^{-3}$; -···-, $k_s/d = 7\times10^{-3}$; -····- , $k_s/d = 20\times10^{-3}$. Szechenyi (1975): ●, $k_d/d = 4\times10^{-4}$; ◆ , $k_d/d = 2\times10^{-3}$. Güven et al (1979): △ , $k_s/d = 2.5\times10^{-3}$; ▽ , $k_s/d = 3.11\times10^{-3}$; ⊕ , $k_s/d = 4.18\times10^{-3}$; ◇ , $k_s/d = 4.18\times10^{-3}$ ($k/d = 3.55\times10^{-3}$); □ , $k_s/d = 6.21\times10^{-3}$. ⊗ , Batham (1973), $k/d = 2.17\times10^{-3}$. Smooth cylinder results: ○ , Güven et al (1979); × , Achenbach (1968); ⊕ , Batham (1973); --- , Jones et al (1969); ⊗ , Roshko (1961); ⊘ , Szechenyi (1975); ⊘ , van Nunen et al (1972). (from Ref. 34)).

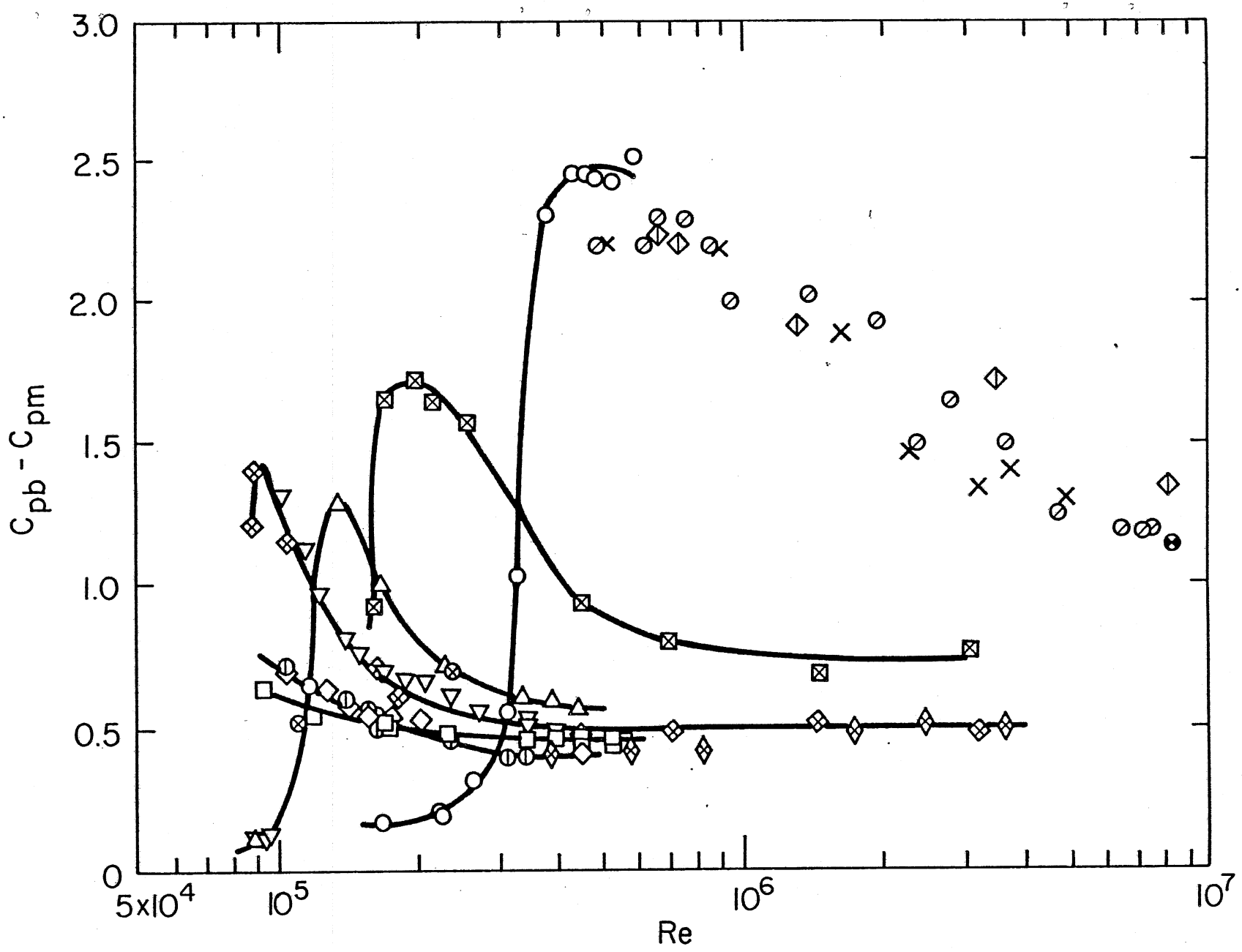

Fig. 3 - Variation of $C_{pb} - C_{pm}$. Cylinders with distributed roughness. Achenbach (1971): ⊠, $k_s/d=1.1x10^{-3}$; ◈, $k_s/d=4.5x10^{-3}$; ⊗, $k_d/d=16.5x10^{-3}$ ($k_s/d=9x10^{-3}$). Güven et al (1979): △, $k_s/d=1.5x10^{-3}$; ▽, $k_s/d=3.11x10^{-3}$; ◍, $k_s/d=4.18x10^{-3}$; ◊, $k_s/d=4.18x10^{-3}$ ($k/d=3.55x10^{-3}$); □, $k_s/d=6.21x10^{-3}$; ⊗, Batham (1973), $k/d=2.17x10^{-3}$. Smooth cylinder results: ○, Güven et al (1979); ×, Achenbach (1968); ⊕, Batham (1973); ◊, Jones et al (1969); ⊗, Roshko (1961); ⊘, van Nunen et al (1972) (from Ref. (34)).

effects, as will be presently discussed, and there may be significant ℓ/d and end condition effects on flow two-dimensionality (see below). The effects of ℓ/d on mean flow parameters have not yet been well documented (see e.g. (25)). In the supercritical Re range and for ℓ/d values between say, 3 and 8, C_d (corrected for blockage) appears to increase with decreasing ℓ/d in solid wall tunnels (25, 34). Even for large ℓ/d ratios, it would appear from results of Humphreys (37) and more recent results of Korotkin (44), that the flow may exhibit a 3-D, cell-like structure along the cylinder span, at least in certain Re ranges. (Mattingly (50) has also found a spanwise periodicity with a wave length of a few diameters, without attempting any quantitative description.)

Actually, indications of spanwise 3-D structures can be found in earlier experimental results: Roshko (62) at Re = 80 (see Gerrard (32) for a discussion of low Re results and additional references), Etkin et al (21) at Re from 2×10^4 to 6×10^4, and Macovsky (48) at $10^4 < Re < 10^5$. (Etkin et al found indirect evidence of spanwise variations, with correlation lengths of about 8d, from an analysis of acoustic radiation measurements, while Macovsky observed large spanwise phase changes occurring at random and increasing in importance as Re approached 10^5.) Humphreys used long, thin silk threads, capable of stretching from the stagnation point ($\theta = 0$) to about $\theta = 130^\circ$, to visualize the flow at Re from 4×10^4 to 6×10^5. At $Re < 10^5$, the threads seemed to present no substantial interference with the flow, flapping in and out with the wake and showing some spanwise irregularity, but without any identifiable pattern. At the onset of the critical regime, $Re \sim 10^5$ (at which Re a well defined vortex street is still present for the bare cylinder), the threads, acting apparently as tripping devices for the cross flow from laminar to turbulent separation regions, produced a distinct spanwise wave or cell pattern, very stable in time, formed of cells with and without reattachment, which made the oscillating lift practically vanish and severely reduced C_d. Characteristic cell sizes were between 1.4d and 1.7d. The threads broadened the critical region of decreasing C_d coefficients, as would an increase in surface roughness. As Re was increased beyond 10^5, the cells remained the same in size, but the boundaries jumped around with greater and greater rapidity, until by $Re \sim 3 \times 10^5$ they could no longer be identified by visual observation.

The silk threads acted evidently as organizing agents for the flow. Similar instances of relatively small disturbances dominating an instability phenomenon to the exclusion of other factors, otherwise important, have been discussed by Morkovin (52). Lateral oscillations of the cylinder at approximately its Strouhal frequency represent incidentally a rather powerful organizing agent, which can increase the spanwise correlation of the vortex shedding and result in an increase in the unsteady lift (see e.g. (14), (33)).

According to Humphreys, however, the same type of cell formation could exist at the lower edge of the critical Re range with the threads removed, in this case without any well-defined periodicity but rather with the cells of turbulence moving about randomly on the cylinder surface, providing the basic mechanism for transition to turbulence in the boundary layer. Incidentally, Humphreys found considerable end-condition effects (in spite of his cylinder model having $\ell/d = 6.56$) in the subcritical Re range, which became less and less pronounced as Re approached the critical range. It should be noted that the evidence for the existence of the moving cell pattern is qualitative in nature, as Humphreys has pointed out.

In a recent investigation, Korotkin (44) found regular and significant mean pressure nonuniformities along cylinder generatrices at angles θ between 90° and 130°, that is, just before and in the zone of separation, for Re of the order of 10^6. (Such regular nonuniformities in mean pressure have not been generally reported in the literature.) By using silk threads in the manner of Humphreys, Korotkin found the same type of honeycomb structure, but at much larger Re, of the order of 10^6 (cylinder $\ell/d = 5$) and also at subcritical Re, of the order of 5×10^4 to 10^5 (cylinder $\ell/d = 25$). While the honeycomb cells at subcritical Re were observed to change their location along the cylinder in intervals of 3 to 8 seconds, at Re $\approx 10^6$, the location of the cells appeared quite stable. Due to the presence of the cells at clearly subcritical Re, Korotkin tends to attribute the 3-D cell-like structure of the flow to the concavity of the streamlines in the vicinity of the separation point, rather than to three-dimensionality associated with transition from laminar to turbulent flow in the separating and reattaching layer, as suggested by Humphreys. With a sharp pointed nose attached to the cylinder so as to reduce streamline concavity near the stagnation point, measured pressure distributions showed the presence of 3-D separation in the separation zone, just as without the nose. Korotkin concludes then that it is the concavity of

the streamlines near the separation point that is responsible for the generation of Görtler vortices, which would be produced both in the subcritical and critical ranges, and which would produce the 3-D cellular disturbance pattern. This would be in agreement with observations of Kestin and Wood (43) which show that the intensity of 3-D disturbances is highest near the separation point, although these authors attributed the generation of vortex-like disturbances to the region near the stagnation point.

The also recent investigation of Sonneville(71) at Re ~ 5×10^4, in which velocity, pressure, and lift and drag cross-correlations and cross-spectra were measured, did not disclose any spanwise nonstationary behavior as described by Korotkin; statistically, the flow was two dimensional, and no phase differences were detected, in the mean, along the cylinder span, thus excluding any hypothesis of organized propagation.

B. Definition of flow regimes

The preceding, somewhat extended discussion of 3-D effects, together with the inherent unsteadiness of the flow around a cylinder, point toward the possible shortcomings of 2-D, steady-mean-flow descriptions, obtained by averaging over times which are large compared to the significant vortex-shedding periods. This is true, in particular, with regard to the definitions given in the preceding section of the various flow regimes: subcritical, critical, supercritical, and transcritical, the boundaries of which still require further investigation.

The transitions which divide the flow regimes are inherently related to transition to turbulence in the wake or boundary layer of the cylinder and to the development of single and double-shear-layer instabilities, as discussed in detail in reviews by Morkovin (52) and Marris (49), and in a paper by Bloor (15). The development of single-shear-layer, inviscid oscillation modes (originally created through viscous action) can be likened to a vortex induction process (52) in which inertially-controlled momentum and vorticity transfers occur in (and as a result of) a uniformly oriented vorticity field, perpendicular to the velocity vector. This process is essentially different from the vortex stretching and distortion of turbulence, brought about by nonlinear acceleration terms which vanish in 2-D flows. Turbulent and laminar shear layers exhibit similar inviscid-instability behaviors, with fast subsequent decays in the case of the turbulent layers due to turbulent mixing.

The double-layer instability responsible for the shedding appears at $Re < 100$ ((52), (49), (15)). Morkovin and Marris assume that in the range $150 < Re < 300$ transition to turbulence occurs in the free shear layers originating from the cylinder prior to their rolling up into vortices (which would therefore be turbulent from their inception). Bloor, on the other hand, in experiments in a low-turbulence wind tunnel ($T_u = 0.03\%$), found that only for $Re > 400$ did transition occur in that manner, being preceded by the basically 2-D Tollmien-Schlichting waves. For $Re < 400$, Bloor found transition to turbulence to occur in the fully formed street and to be associated with basically 3-D irregular fluctuations. For brevity, the remainder of this review will be restricted to flows at Re larger than at least 10^4; the reader is referred to the three papers cited above and to papers by Gerrard (31), (32) and Roshko and Fiszdon (63) for accounts of events at lower Re.

Laminar separation as described in the preceding paragraph, obtains up to Re of about 10^5: the large-scale double-layer instability exhibits a turbulent fringe but the initial segments of each layer are laminar and present secondary, small-scale vortices (single-sheet instabilities). These secondary vortices could affect the necessary lateral momentum transfer to reattach the separated layer, forming a long laminar (pulsating) bubble (52), (77). Alternately, the momentum transfer needed for reattachment could be provided by transverse turbulent fluctuations, in which case a short (laminar separation-turbulent reattachment) bubble is formed. In either case, final separation is pushed downstream, leading to narrower wakes and much smaller wake suctions and drag coefficients (see Fig. 1).

The critical regime thus develops, the transition from the subcritical Re range occurring at Re between 10^5 and 3×10^5. The exact sequence of events at this first or lower transition is still not completely elucidated. In the subcritical flow range the boundary layer on the cylinder (laminar) separates at approximately $\theta = 80^\circ$ over a considerable range of Reynolds numbers, up to about $Re = 10^5$. (The drag coefficient, C_d, exhibits a plateau over the same Re range.) According to Achenbach (2, 4), over the Reynolds number range from 1.2×10^5 to 3×10^5, the angle of separation, θ_s, changes from 80° to about 110° with the boundary layer separating always in laminar fashion, this change being of course accompanied by an increase in base pressure and a considerable drop in C_d (see Fig. 1). Only at $Re = 3 \times 10^5$ the phenomenon of the laminar separation-turbulent reattachment

bubble would occur, the laminar boundary layer separating at $\theta_{s,lam} = 105^{o}$ and reattaching immediately as a turbulent layer, with final separation occurring at $\theta_s = 140^{o}$. The reader is referred to Achenbach's original papers for the physical arguments and data supporting these views. Here we point out only that over the range from $Re = 1.2x10^5$ to $Re = 3x10^5$ (the critical Re according to Achenbach's definitions, where C_d exhibits a minimum) a long laminar bubble in the sense of the preceding paragraph could well be generated which could account for the downstream motion of the separation point as observed by Achenbach. We denote (with Achenbach) the range of Re from about $1.2x10^5$ to the Re at which the bubble disappears (but leave this Re undefined except to say that it would be of the order of 10^6) as the critical Re range (see Fig. 4). In this transitional range (this would probably be a better name for it actually), the flow is very sensitive to any disturbances, which may explain the large variations in experimental data from different investigators.

The supercritical flow range as defined here begins at the second or upper transition, where the bubble disappears (Re of the order of 10^6). It is characterized by transition to turbulence in the boundary layer occurring ahead of separation and moving upstream toward the point of stagnation as Re increases. Transition occurs first downstream of the main cross section (transition angles $\theta_T > 90^{o}$). Once transition occurs ahead of the main section, it rapidly shifts toward the stagnation point with increasing Re (2, 35). It should be noted that according to Achenbach's definitions the transcritical range would begin at the Reynolds number that gives $\theta_T = 90^{o}$. The definition tentatively adopted here for the transcritical flow range seems more significant from a physical point of view; it is, however, asymptotic in nature. Roshko's (61) original definition of the transcritical range embodies both the present supercritical and transcritical regimes; the word "postcritical" has also been used in the literature to denote these two ranges. A universal terminology is needed to avoid confusing statements. We note in particular that the word transcritical has also been used in the literature to denote the critical Re range (73).

We note finally that the fall of the tangential stress on the cylinder surface (as a function of θ) to a minimum and subsequent immediate rise to a maximum, which characterize the laminar separation-turbulent reattachment

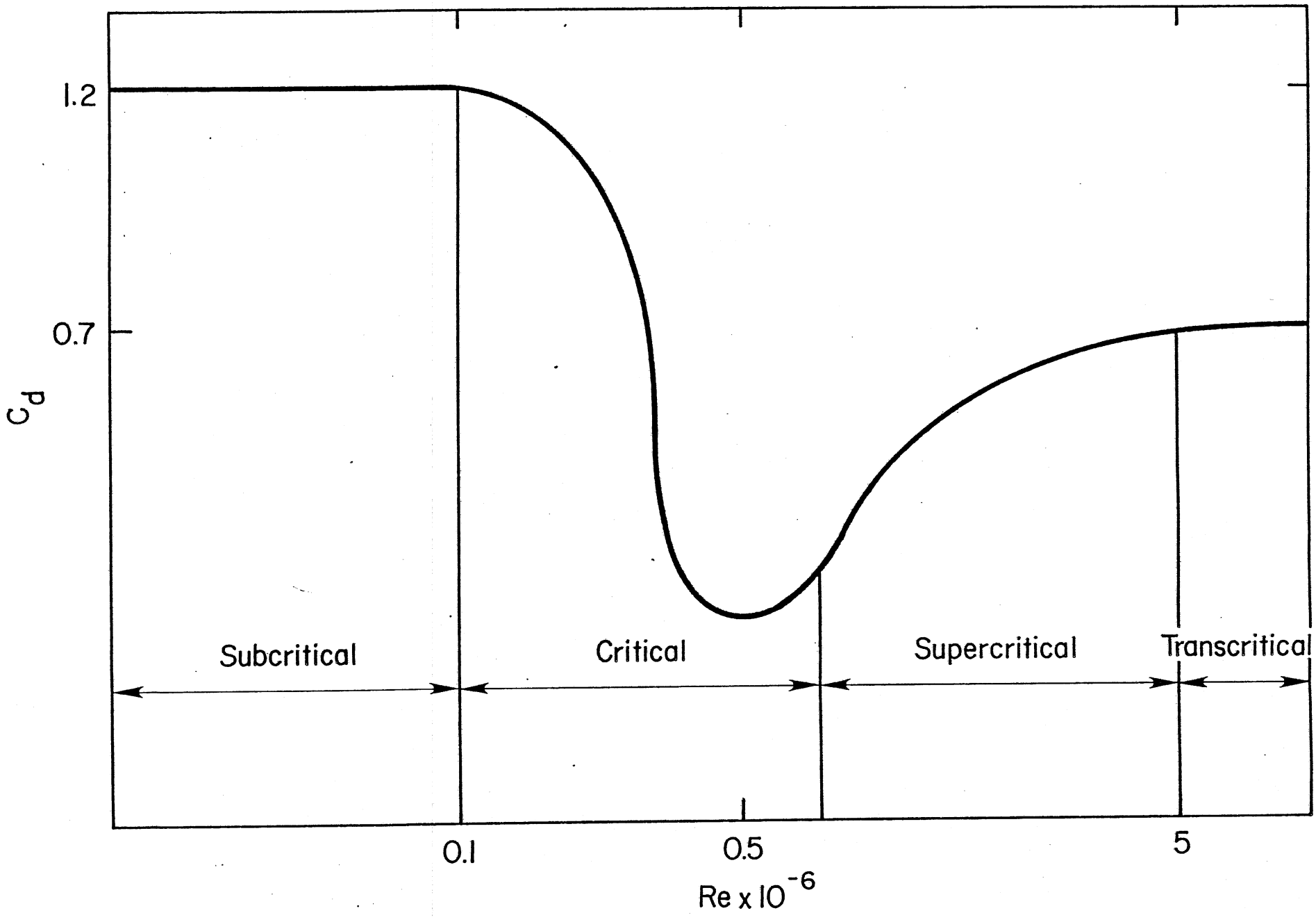

Fig. 4. Tentative definition of flow regimes. Reynolds numbers and C_d values shown are for illustration purposes only.

bubble, can be seen in the experimental results of Fage and Falkner (23) obtained using skin-friction tubes, dating back to 1931 and preceding Achenbach's (4) by 37 years.

C. Unsteady loads

While the dependence of the mean pressures on both Re and surface roughness has been the object of several studies for both cylinders and cooling towers (e.g. (1), (26), (34), (57)), corresponding studies for parameters characterizing the fluctuating loads (Strouhal number S, root-mean-square lift, drag, and pressure coefficients, respectively C'_L , C'_d , and C'_p , and more generally the correlations and spectra of the fluctuations) are in general still needed, in particular for critical, supercritical, and transcritical Re (a recent contribution is (59) where cooling-tower model and prototype data are reported). The information available shows that the dominant subcritical spectral peaks disappear or are greatly reduced in level of sharpness in the critical Re range (8, 11, 30, 41, 77). The disappearance of regular shedding is very likely due to the strong flow three-dimensionality introduced by turbulent spots or bursts originating in the (transitional) laminar boundary layers ahead of the separation bubbles, which disrupt the bubbles asymmetrically (41), leading to small axial correlations along the structure and to appreciable axial non-uniformities, which in turn result in a breakdown of the double-layer instability responsible for the alternate shedding (8, 11, 41). The regular shedding reappears (41, 61, 73, 76) as the boundary layer becomes turbulent prior to separation, the bubbles disappear, and axial homogeneity is recovered (supercritical and transcritical Re ranges). The variation of S with Re sketched in Fig. 1 is in agreement with these ideas, the difference in S for subcritical and supercritical flows being due to the different wake widths.

These ideas make the disappearance of regular shedding dependent on the turbulence characteristics of the stream and on surface roughness. Vortex shedding could continue after the bubble regime appears if disturbances are minimized, with larger S values due to the much narrower wake (11, 60). (Bearman's (11) measurements show that the velocity fluctuations in the wake in the one- or two-bubble regime have sharp spectral peaks, but with much smaller power at the Strouhal frequency than at a typical subcritical Re. However, only very weak velocity fluctuations at the shedding frequency were

observed near the cylinder surface at $\theta = 90^{o}$, which is consistent with the increase in the bandwith of the peaks of the lift fluctuation spectra in (60) as Re approached and passed the critical Re). The disappearance of the bubble may result in abrupt changes in the parameters (as reported in (4) for the separation angle, θ_s), but the available data are not sufficient to determine any functional dependence on Re accurately.

The preceding ideas are not inconsistent with Humphrey's (36) and Macovsky's (48) findings concerning the three-dimensionality of the flow as Re approached the critical range. However, the possible three-dimensionality of the flow in the subcritical Re range suggested by the results of Korotkin (44) casts doubts that require additional investigation for their elucidation.

For subcritical Re, with coherent shedding and sharp spectral peaks, C_p' presents a maximum around $\theta = 80^{o}$ (θ = angle from leading generator) of the order of 0.40, decreases to about 0.30 at $\theta \doteq 120^{o}$, and then increases again somewhat in the wake region, presenting another maximum at about $\theta = 160^{o}$ ((71), Re = 45,000; (72), Re = 40,000). The increase in the wake region is not present in the data of Bruun and Davies (16) at $Re = 2.4 \times 10^{5}$ (still subcritical, low turbulence stream) which give $C_p' \sim 0.20$ at $\theta = 180^{o}$, nor in the data of Batham (8) at $Re = 1.11 \times 10^{5}$ where, on the other hand, an additional peak at $\theta \sim 105^{o}$ following the maximum at $\theta = 80^{o}$ can be seen. Batham interprets the presence of these two peaks as indicating the formation of a separation bubble. However, the high vortex-shedding levels at Strouhal numbers of about 0.2 exhibited by the corresponding spectra (which result in high C_p' values around separation) and the typically subcritical mean pressure distribution would appear to indicate that the critical range has not been reached, although this would leave the second peak unexplained. It is interesting to note that at $Re = 2.4 \times 10^{5}$ (smooth cylinder), Batham detected strong shedding at $\theta = 60^{o}$ and $\theta = 90^{o}$, but not at $\theta = 75^{o}$. Since Batham rotated his cylinder, he interprets this as implying transition to critical flow due to small changes in roughness resulting from the rotation. Indeed, transition phenomena are highly sensitive to small surface disturbances (11, 30, 70) and to freestream turbulence (11, 16). In addition, end and wall confinement effects can be particularly significant at transitional Re (22, 25, 30, 70), to the point of resulting in serious nonuniformities along the cylinder span (76), and all these factors must be considered in any data comparison, including possible flow asymmetries (see in paritcular (11), (58)).

At Re = 45,000 Sonneville (71) has determined by spectral analysis the major components of the fluctuating pressures on the cylinder surface. His conclusions are in agreement with earlier data of Surry (72) and Bruun and Davies (16). Most of the pressure fluctuation energy for $\theta < 160^{\circ}$ comes from a frequency band around the Strouhal frequency, f_s. This component, which vanishes near $\theta = 180^{\circ}$, appears as a signal with a dominant frequency exhibiting strong low-frequency amplitude modulations. A component at frequency 2 f_s, weak in relation to the total fluctuation, can be seen in the spectra at angles $\theta > 60^{\circ}$. Its energy decreases rapidly away from $\theta = 180^{\circ}$, where it has a maximum. A very weak component at frequency 3 f_s can also be seen in the spectra, in particular near separation. All spectra (except perhaps around the stagnation line) present a low-frequency plateau, increasing in importance toward the back of the cylinder, which Sonneville has shown is directly related to low-frequency modulations of the shedding. These modulations are associated with slow changes in the region of formation of the vortices, that is, with slow evolutions of the shedding mechanism, at frequencies 10 times slower than the shedding frequencies themselves. More precisely, the continuous part of the spectra, important in particular at low frequencies, can be considered as having contributions from two components, one with weak longitudinal correlations, due to the flow turbulence (which in the wake region exhibits considerable broad-band high frequency fluctuations ((16), Re = 2.4×10^5; (72), Re ~ 4×10^4), the other with longitudinal correlations of the order of the correlations of the f_s component. The latter contributes significantly to the longitudinal correlations and, because of its direct relationship to the modulations of the vortex-shedding fluctuations, it can be viewed as characterizing the three-dimensionality of the flow, together with the analogous phase modulations along the cylinder and the relative instability of the Strouhal frequency as depicted by the width of the peaks.

It is interesting to note that hot wire traverses at distances from the cylinder wall of 0.013 d, 0.021 d, and 0.050 d, showed that in the turbulent region $110^{\circ} < \theta < 140^{\circ}$, immediately after (in the sense of increasing θ) the separated shear layers, the velocity fluctuations exhibited fully turbulent spectra, the turbulence apparently masking completely the Strouhal fluctuations (peaks not visible in the spectra). The longitudinal velocity correlations in this zone were accordingly negligible, which was not the

case for the pressure correlations, which remained of the same order of magnitude as the pressure and velocity correlations at angles $\theta < 90^{\circ}$.

The fluctuating lift in the subcritical range has peak values of the order of the steady drag. Keefe (42) measured (sectional) $C'_L \sim 0.46$ at $Re = 5 \times 10^4$, with $C'_d \sim 0.04$, an order of magnitude lower. Sonneville (71) obtained $C_L \sim 0.50$ at about the same Re (both by integration of pressures and by estimation of local values from force measurements for the whole cylinder length, using a correlation function estimate obtained on the basis of his data and data of Surry (72)), and $C'_d \sim 0.13$, much larger than Keefe's C'_d. For brevity, the reader is referred to Sonneville's report for a comparative analysis of C'_L data at $Re < 10^5$, including results of McGregor (51), Humphreys (37), Keefe (42), Bishop and Hassan (13) (flume measurements), and Gerrard (32). Excluding Gerrard's results, which are totally different from the others (Gerrard has conjectured that this may be due to the very low free stream turbulence level of his wind tunnel), the trend that emerges from Sonneville's analysis is that C'_L increases as Re increases from $.5 \times 10^3$ to about 6×10^4, rather rapidly between 5×10^3 and 10^4 (the reasons for this rather steep increase are not clear), and then decreases as the critical range is approached. There is a plateau-like maximum, say between 4×10^4 and 6×10^4, with a value of C'_L between 0.45 and 0.50.

Regarding the C'_d values, Sonneville has noted that Keefe's $C'_d \sim 0.04$ represents only the energy at frequencies around the second harmonic, $2 f_s$, of the Strouhal frequency, at which the drag spectra present a wide-band peak. While the spectral density of the lift presents two peaks, one at f_s, the other at $3 f_s$, with practically all the energy concentrated at the Strouhal frequency, most of the energy of the fluctuating drag is concentrated over the low-frequency range, where the spectra present a plateau for Strouhal frequencies less than 0.02. The contribution from this low-frequency range to the root-mean-square value of the fluctuating drag is generally 3 times larger than the contribution from the peak at $2 f_s$. There is no low-frequency contribution, however, to the fluctuating lift, confirming the symmetry of the low-frequency components of the pressure fluctuations. As with the pressure, the low-frequency component of the drag fluctuations is associated with the low-frequency modulations of the vortex shedding fluctuations at f_s and $2 f_s$.

Batham's (8) results at $Re = 1.1 \times 10^5$ are $C'_L \sim 0.33$, $C'_d \sim 0.1$. Pressure fluctuation correlation lengths, L^p, at $\theta = 90^\circ$ ($T_u < 0.5\%$) from various sources (16) appear to decrease linearly with increasing Reynolds number (with some scatter) from about 4d at $Re = 10^4$ to less than 3d at $Re = 2 \times 10^5$. Surry's (72) measurements at $Re \sim 4 \times 10^4$ ($T_u = 2\%$) show correlation lengths of about 4d between $\theta = 30^\circ$ and $\theta = 60^\circ$, decreasing to about 3.25 d at $\theta = 120^\circ$. At the rear of the cylinder the correlation lengths drop sharply, consistent with the vanishing of the Strouhal frequency component of the pressure fluctuations toward $\theta = 180^\circ$.

Narrow-band correlations can be used to isolate the longitudinal coupling of the vortex shedding phenomenon from the masking effects of free stream turbulence. They can be determined by correlating at two lateral stations the pressure fluctuations corresponding to a frequency band around f_s (correlation of the peak at f_s (71)), or by measuring the ratio of cross spectrum to power spectrum, which for any pair of lateral stations will exhibit peak coherence at the vortex shedding frequency (coherence at f_s). Surry's data (72) show narrow-band correlation lengths, L^p_s, about double the complete correlation lengths cited in the preceding paragraph (see also the discussion of turbulence effects later). These values seem somewhat high when compared with Sonneville's correlation measurements for a longitudinal spacing $\Delta y = 1.9$ d, which show the coherence at f_s to be about 20% to 30% higher than the complete correlation at angles θ between 30° and 120°. But the higher free stream turbulence in Surry's experiments may account at least in part for the difference. Earlier measurements of pressure correlations by Prendergast and velocity correlations by El Baroudi (see (70), (72) for references and comments) produced respectively L^p values of about 4d and 6d at $Re = 45000$. Experimental discrepancies over the correlation lengths are still seen to exist then even in subcritical flow. The phase between the fluctuations at f_s as measured by Sonneville, for $\Delta y = 1.9$ d, is zero on the average (no organized propagation in the spanwise direction).

In the critical Re range C'_p is considerably smaller than in the subcritical range (8, 16) and so is C'_L (8, 30, 60, 70, 73), consistent with the disappearance of organized shedding. Fung's (30) C'_L values

(see Fig. 1: these values represent forces over a cylinder section of length about 1.75 d) are fairly constant ($C'_L \sim 0.135$) for $3 \times 10^5 < Re < 1.4 \times 10^6$. Batham's (8) values (sectional) are somewhat smaller: $C'_L \sim 0.09$ at $Re = 2.39 \times 10^5$ (smooth cylinder) and also at $Re = 1.11 \times 10^5$ (rough cylinder). (See discussion below of Batham's rough-cylinder results.) Schmidt's (70) measurements at Re around 5×10^5 show fluctuating lift values about one-third of Fung's, a difference that could be due at least in part to differences in surface roughness and possible end effects (free-end versus gap effects; see (70) for a detailed discussion). Szechenyi (73) measured unsteady lift coefficients on smooth cylinders which decreased somewhat from $C'_L \sim 0.09$ at $Re = 6 \times 10^5$ to $C'_L \sim 0.06$ at $Re = 4 \times 10^6$. Although there is obviously some scatter in the data, which could be due to end-condition and small-disturbance effects, the drastic reduction in C'_L values from the subcritical to the critical Re ranges is clear. Neither Fung nor Schmidt detected any significant shedding in the spectra (up to $Re = 1.4 \times 10^6$ in Fung's case). The quasi-random spectra of Szechenyi (73) show at most a weak shedding-frequency component, insufficient to determine a value of S, in what Szechenyi calls the transcritical flow regime following the usage of the prefixes in aerodynamics (the present critical range). Batham's results are a little more difficult to assess because only two Re were investigated. According to the discussion here and Batham's description, both the smooth-cylinder results at $Re = 2.4 \times 10^5$ (recall the earlier discussion of these results) and the rough-cylinder results at $Re = 1.1 \times 10^5$ are probably in the beginning of the critical range. In particular, considerably reduced vortex shedding levels, accompanied by marked reductions in the C'_p and C'_L coefficients, were observed by Batham in the latter case.

Axial length scales for the fluctuating lift in the critical range are generally less than one diameter (70). Pressure correlation measurements of Prendergast (cited in (70)) show clearly the decrease in correlation lengths as the transitional Re range is approached, in agreement with the disappearance of organized shedding. The unsteady drag coefficient, C'_d, decreases as C'_L with increasing Re and has rather small values in the critical range, of the order of a few per cent (8, 30, 58, 60, 70), consistent with Sonneville's finding that the low-frequency modulations of the vortex shedding contribute a large percentage of the energy in the drag fluctuations.

Richter and Naudascher's (60) investigation of the effect of large blockages on the flow in the critical Re range disclosed the same sharp increase in Strouhal number reported by Bearman (11) as the separation bubble appeared, for all blockage ratios investigated. The sharpness of the increase compared to the relatively more gradual variation of other parameters prompted the authors to suggest its location as a definition of the critical Re (at which the critical range begins). Related to Bearman's observation that the power at the Strouhal frequency was 33 db down, after transition, on the power at a typical subcritical Re, is Richter and Naudascher's plot of a frequency band, Δ, around f_s which contains a given percentage of the total r.m.s. lift fluctuations. As Re increases through the critical range, Δ increases markedly, and so does the degree of randomness of the fluctuations. For a confinement ratio of 25%, Richter and Naudascher's measurements give $C'_L \sim 0{,}04$, $C'_D \sim 0.01$ (rather small values), and $S = 0.43$ ($S = 0.46$ in Bearman's (11) measurements).

Richter and Naudascher note that the decrease in C_D, C'_L and C'_D as Re reaches into the critical range is more gradual than the sharp increase in S. This suggests an increasing three-dimensionality of the flow along the span, as Re increases, before the bubble forms. (As noted earlier, Achenbach (2) has suggested that the bubble appears only when C_D reaches its minimum.) The fluctuating drag is more sensitive to this three-dimensionality than either the fluctuating lift or the mean drag, and thus the decrease in C'_D starts at lower Re.

The re-establishment of the narrow-band shedding in the supercritical range for a polished cylinder ($k_s/d \sim 0.2 \times 10^{-5}$) is rather gradual according to the unsteady lift measurement of Jones et al (41), who have grouped the lift forces on the cylinder into three regimes according to the shape of the auto-correlation and power spectral functions of the fluctuations: wide-band random (auto-correlation function has no more than one peak other than the peak at zero delay, $1.1 \times 10^6 < Re < 3.5 \times 10^6$), narrow-band random (two or more consecutive peaks in the auto-correlation function, percentage decrement between peaks greater than 10%, $3.5 \times 10^6 < Re < 6 \times 10^6$), and quasi-periodic (percentage decrement between consecutive peaks in auto-correlation function less than 10%, $Re > 6 \times 10^6$). The corresponding Strouhal bandwidth (defined as the frequency interval between the half-power points of the spectrum peak) is large (e.g., 0.15) in the wide-band

random regime and narrows rapidly as Re increases from 3.5×10^6 to 6×10^6, with a typical value of 0.02 at $Re = 9 \times 10^6$. The reappearance of shedding at large Re as first observed by Roshko (61) in the wake of a sand-blasted cylinder ($k_s/d \sim 10^{-5}$) was quite sudden, at $Re = 3.5 \times 10^6$. Below this Re the signal from a hot wire 7.3 diameters downstream from the cylinder axis and 0.7 diameters off the centerline presented no peak frequencies; above, a strong spectral peak appeared together with the lower double-shedding-frequency peak, typical of subcritical flows near the centerline behind the cylinder.

A few results concerning frequency characteristics of fluctuating quantities in the supercritical (and transcritical) flow range are available in terms of Strouhal numbers (rather than Strouhal bandwidths) and can be compared (see Fig. 5). Roshko's (61) S values are approximately between 0.26 and 0.28 (increasing with Re) for $3.7 \times 10^6 < Re < 8.4 \times 10^6$. Jones el al values ((41), Mach number 0.3 or 0.2) show a larger increase with Re in the (narrow-band random) range $3.5 \times 10^6 < Re < 6 \times 10^6$, reaching $S = 0.3$ and appearing to remain constant up to $Re = 1.4 \times 10^7$. The rough-cylinder results of Szechenyi (73, 74, 75) (see Fig. 5(b)), to be discussed more fully presently, asymptote at about $S = 0.26$ for large Re for all roughnesses investigated. (It should be noted however that Szechenyi's measurements in a smaller, higher T_u wind tunnel yielded values of S roughly 25% lower, a difference which remains unexplained according to Szechenyi.) For the larger roughnesses ($k/d \sim 10^{-3}$) the asymptote is approached clearly from larger S values, up to $S = 0.3$. Szechenyi's smooth cylinder results show $S \sim 0.3$ at $Re \sim 5.7 \times 10^6$; the trend for larger Re is not defined by the data. Spectral peaks at large Re are shown also by the data of Warschauer and Leene (81) (cantilevered cylinder in a water tunnel, bending oscillations possible) and Pröpper (59) (prototype cooling-tower measurements) but quantitative comparison with these results is not possible because of the different experimental conditions and/or different geometries. Tani (76) has reported achieving supercritical flow conditions at $Re = 6 \times 10^5$ through use of trip wires, with Strouhal numbers around 0.30 (See Fig. 5 (a)). Regular shedding has been achieved also by Nakamura (54) at Re from about 2×10^5 to 2×10^6 using large surface roughnesses (1.5 and 5 mm beads, $k/d \times 10^3 = 2.5$ and 8.5, respectively) and roughness strips made with the

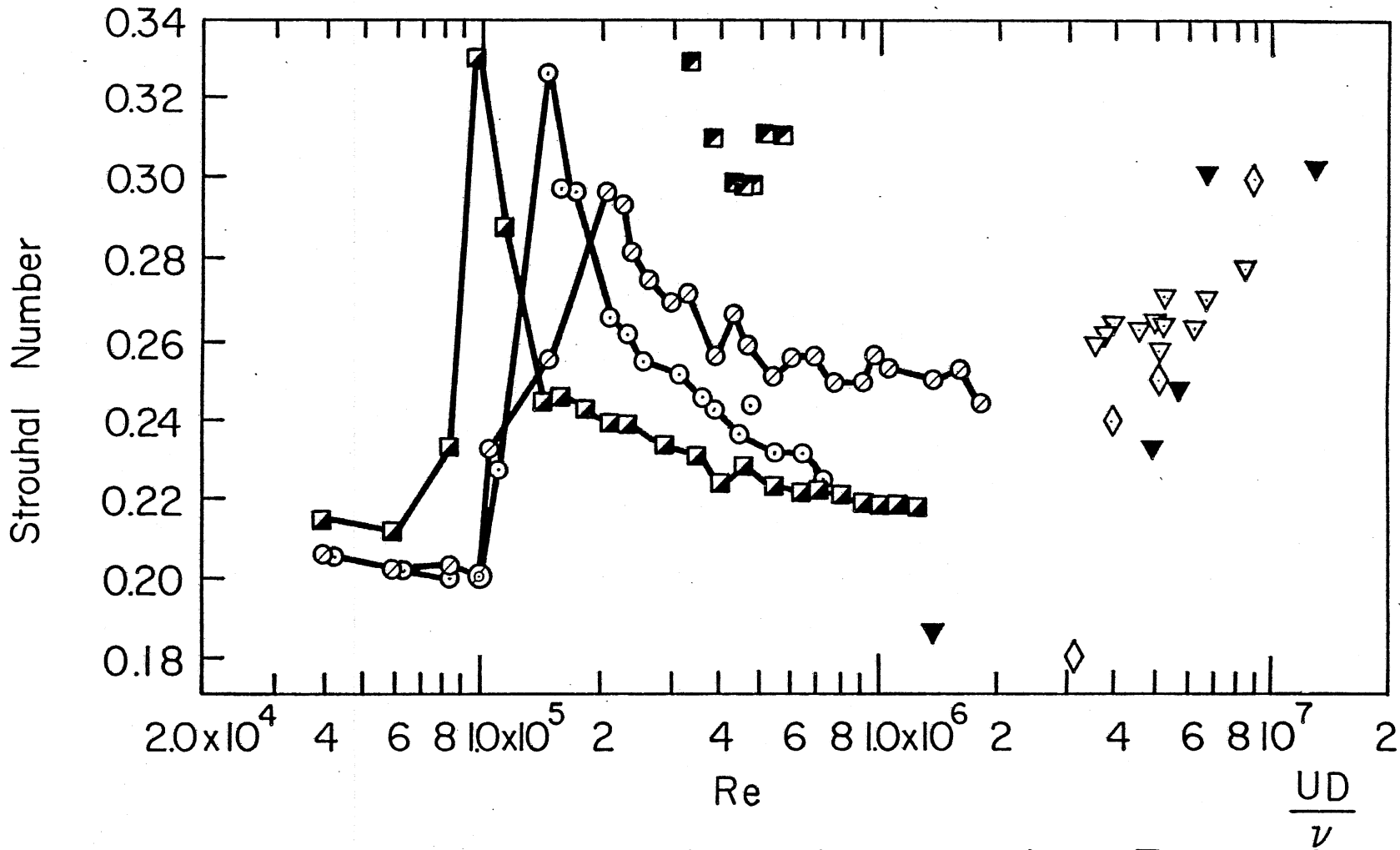

Fig. 5(a) - Strouhal numbers after reappearance of organized shedding. Smooth cylinders: ▽, Roshko (61); Jones et al (41) (results in region of definite vortex shedding): ▼, M = 0.3; ◊, M = 0.2. Roughened cylinders: Nakamura (54): ○, dist. roughness, $k/d = 2.5 \times 10^{-3}$; ◪, dist. roughness, $k/d = 8.5 \times 10^{-3}$; ⊘, roughness strips; ◪, Tani (76).

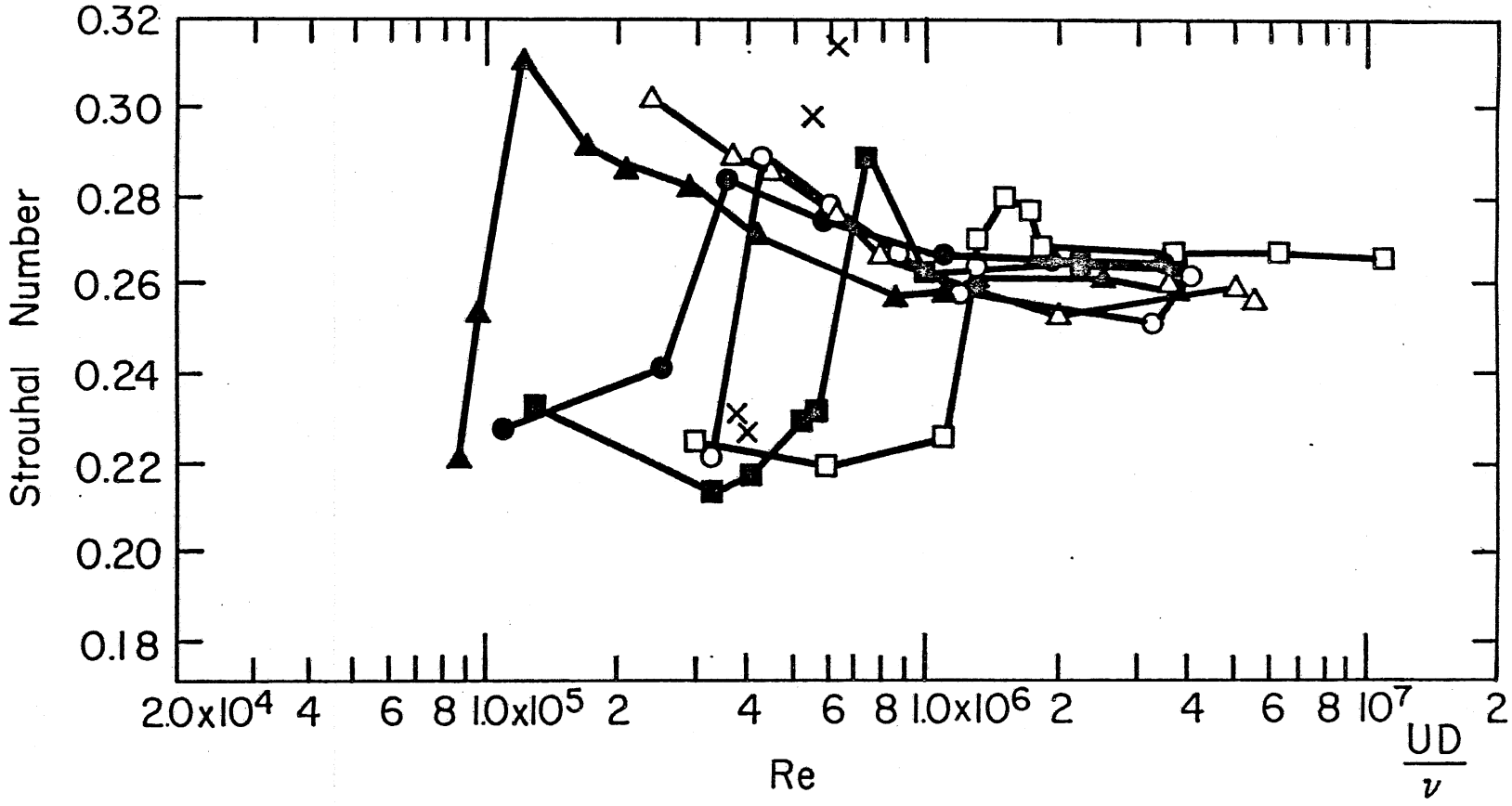

Fig. 5(b) - Strouhal numbers after reappearance of organized shedding. Data of Szechenyi (74): x, smooth cylinder; □, k/d = 1.5×10^{-4}; ■, k/d = 2.5×10^{-4}; ○, k/d = 5×10^{-4}; ●, k/d = 7.5×10^{-4}; △, k/d = 10^{-3}; ▲, k/d = 1.75×10^{-3}.

1.5 mm beads (strip width 2 cm, $k/d = 2.5 \times 10^{-3}$, angular position 50°). The Strouhal numbers, which appear to asymptote at 0.22 (distributed roughness) and 0.25 (strips), are somewhat smaller than those quoted above, and Nakamura tends to attribute this discrepancy to possible end condition effects, as a value of $S = 0.27$ was obtained for the distributed roughness by sealing the cylinder end gaps.

For smooth cylinders in the critical range $0.3 \times 10^6 < Re < 3 \times 10^6$, the data exhibit no distinct spectral frequencies, and most investigators had difficulty in obtaining an identifiable dominant frequency (but see earlier discussions of the results in (11) and (60)). This probably may be the reason for the poor agreement in the results of the few investigations reporting Strouhal number data in this range, which include Relf and Simmons and Delaney and Sorensen (Refs. in Jones et al (41); see also the discussion in Roshko (61)), Spitzer (cited by van Nunen et al (58)), van Nunen et al (58), and Bruun and Davies (16)). The peaks in the spectra in these investigations, when present, probably have little energy associated with them, in agreement with the results of Fung (30), Ezra and Birnbaum (22), and Schmidt (69, 70) already cited, in which no peak S values could be identified in the critical range. Still, some unexplained experimentally-determined spectral peaks at S values which do not fall within the present framework of ideas, remain (see e.g. (58)).

Schmidt (69) extended his data up to $Re = 5 \times 10^6$ without encountering any dominant periodicity. Similarly, Buell et al's (cited by van Nunen et al (58)) pressure fluctuation measurements on a missile-type model at $2.2 \times 10^6 < Re < 6.2 \times 10^6$ disclosed no dominant periodicities. These results reach into Jones et al's narrow-band random regime, but in both cases there are differences in geometry, in particular because of the possibility of a tip effect, and the process of recovery of organized shedding could be quite sensitive to small differences in flow and model conditions.

As the shedding reappears in the supercritical range, C'_L should increase (55) (in the subcritical range most of the energy of the lift fluctuations was concentrated at the Strouhal frequency). While the data of Jones et al (41) and van Nunen et al (58) do not bear out this expectation (see Fig. 1(b)), Szechenyi's (73, 74) and Batham's (8) measurements

on rough cylinders show $C'_L \sim 0.09$ in the critical range, increasing to $C'_L \sim 0.26$ at transcritical Re (see below for discussion). The magnitude of unsteady lift as measured in (41) shows a very large scatter at Re from 1.4×10^6 to about 8×10^6 (in both the side-band random and narrow-band random regimes, extending somewhat into the quasi-periodic regime) with values between about 0.06 and 0.14, of the order of Schmidt's (69) C'_L values and somewhat smaller than Fung's (30) critical range values. Actually, C'_L appears to be multiple-valued, a condition that Jones et al attributed to possible flow asymmetries. The C'_L data of van Nunen et al (58) fall broadly within the region of multiple-valuedness of Jones et al's data: force-balance measurements are scattered between about 0.06 and 0.14, pressure-integration measurements between about 0.04 and 0.08. It should be noted that van Nunen et al found either no dominant peaks or very weak ones in velocity, pressure and lift (and also drag) fluctuation spectra, in the range $0.6 \times 10^6 < Re < 6.9 \times 10^6$. At $Re = 7.25 \times 10^6$, again only rather weak peaks were observed (at $S \sim 0.27$) in the lift and pressure spectra. The contrast with the strong peaks in the results of Jones et al (41) and in the other references in Fig. 5 is striking. We note finally that Nakamura's (54) results at $Re = 8.5 \times 10^5$ were $C'_L \sim 0.14$ for $k/d = 8.5 \times 10^{-3}$ and $C'_L = 0.05$ for the roughness strips at 50^o with $k/d = 2.5 \times 10^{-3}$, suggesting fairly different vortex shedding strengths in the two cases.

Supercritical flow was achieved at relatively small Re in the experiments of Szechenyi (73, 74), Batham (8) and Nakamura (54) by increasing the surface roughness of the cylinder models (27, 28, 34). (Tani (76) used trip wires for the same purpose; Nakamura used also roughness strips.) Szechenyi gives a clear picture of the re-establishment of vortex shedding at large Re: the quasi-random spectrum characteristic of the critical range (which he calls transcritical) changes to a spectrum with a clear and dominant peak at the shedding frequency. For $k/d = 10^{-3}$, for example, the peak reappears at $Re \sim 2 \times 10^5$. Szechenyi observed further that at sufficiently high Re so that the flow was supercritical increasing k/d beyond a certain limiting value broke up the single well-defined peak at the shedding frequency; the roughness particles were apparently so large that they disturbed the axial uniformity of the flow and disrupted the coherent shedding. (Nakamura (54) did not observe this phenomenon.) Incidentally, the interrelationship between coherent shedding and axial flow

uniformity has been examined at certain length by Naumann and Quadflieg (55, 56), who investigated several types of 3-D disturbances, among them stepped (axial) separation wires with variable angular distances between them, cylinders with tapered and step-like changes in cross-sectional diameter, and cylinders with a free end. In particular, corrugated or broken separation wires were found to prevent effectively coherent shedding in all cases investigated, these results being consistent with the use of helical stakes on rounded stacks to reduce or prevent oscillations (14).

The r.m.s. lift coefficient, C'_L, is given by Szechenyi in terms of the roughness Reynolds number, $Re_k = Uk/\nu$. The data covers a fairly broad band, increasing from about 0.09 ± 0.02 in the critical range to about 0.26 ± 0.02 in the transcritical range, leveling off at $Re_k \sim 1000$. (The envelope of the experimental results corresponding to the asymptotic values of C'_L is shown in Fig. 1(b).) A discussion of the analogous presentation given by Szechenyi for his steady drag data and of the role of the parameters Re and k/d (Re_k = Re k/d) has been given in (34) and is not reproduced here. The difference between the transcritical ($C'_L \sim 0.26$) and subcritical ($C'_L \sim 0.50$) lift coefficients is very likely due to differences in the strength of the shed vortices (55) related to the different separation angles and wake widths which obtain in the two regimes. But the general disagreement in C'_L values in the supercritical regime requires further investigation of these effects.

Other than Batham's (8) rough cylinder results at $Re = 2.4 \times 10^5$ (probably at the beginning of the supercritical range, see below) no pressure fluctuation measurements for supercritical flow seem to be available. As for subcritical flow C'_p presents a maximum in the region near separation. The C'_p levels at the two Re investigated by Batham, 1.1×10^5 and 2.4×10^5, are not very different (maxima about 0.15, slightly higher at the larger Re, but occurring as separation about 15^o further back). The C'_L values show a change from 0.09 at the smaller Re to 0.15 at the larger Re, consistent with the considerably increased vortex shedding level observed by Batham in the corresponding spectra, which he ascribes to transition being more nearly complete at the separation point and the boundary layer more homogeneously turbulent (axially).

Because of the large surface roughness the transition from a laminar boundary layer prior to separation, to a turbulent one, may occur somewhat differently than for a smooth surface (in particular, a bubble may not appear (1)), but the results point toward $Re = 2.4 \times 10^5$ being supercritical for $k/d = 2.17 \times 10^{-3}$, which agrees with Szechenyi's results. The measured Strouhal number of 0.23 at $Re = 2.4 \times 10^5$ is somewhat low compared to data already cited. The measured lateral correlation scales are large, of the order of the subcritical values, due to the shedding: $L^P = 4d$ at $\theta = 30^\circ$, decreasing to about 3d between $\theta = 60^\circ$ and $\theta = 150^\circ$ (at $Re = 1.1 \times 10^5$, L^P ranges from 2d at $\theta = 60^\circ$ to less than d at $\theta = 150^\circ$). Szechenyi (73) calculated lateral lift correlation scales of the order of 9d, exceedingly large.

The pressure fluctuation measurements of van Nunen et al (58), at Re up to 7.25×10^6, although nominally extending into the supercritical Re range, are associated with spectra with rather weak peaks, in contrast with the results of Jones et al (41) and other results mentioned earlier. The C_p' distributions show a peak in the region near separation, at $\theta \sim 120^\circ$, for $0.48 \times 10^6 < Re < 0.76 \times 10^6$, of the order of 0.15. The peak disappears at somewhat higher Re, to reappear again at $Re = 2.69 \times 10^6$. At $Re = 7.25 \times 10^6$, a maximum C_p' of the order of 0.20 at $\theta \sim 100^\circ$ can be seen in the distributions. The significance of these results, in the absence of strong shedding, is not clear. Consistent with this absence (see discussion of critical values) are the low values of C_d' measured by van Nunen et al (58), about 0.02 at $Re > 4 \times 10^6$. Batham's (8) rough cylinder results show little change in C_d' from $Re = 1.1 \times 10^5$ ($C_d' \sim 0.032$) to $Re = 2.4 \times 10^5$ ($C_d' \sim 0.037$). All these values are much lower than the subcritical values.

Cross correlation measurements are obviously needed at large Re and/or with large roughness to resolve existing discrepancies and to map fully the characteristics of the flow and the unsteady loading in the supercritical range. Incidentally, the criterion $Uk/\nu > 200$ proposed in (73) as a condition for supercritical flow does not appear to be supported by the results in (41) and (61), even taking into account the uncertainty in the definition of k, and its validity should be tested further. A sharp definition of the boundary between critical and supercritical flow probably required a Strouhal band width criterion (41, 60) to characterize the spectral peaks.

FREE STREAM TURBULENCE EFFECTS

The interest of the study of the relationship between the turbulent inputs to a body and the resulting forces and pressures on it resides in the application to the prediction of the response of a structure to atmospheric turbulence. Relatively few experimental studies are presently available, however, for large rounded structures in general (and for other large bluff bodies as well). Theoretical analyses are even fewer. In the case of lattice structures, such as guyed and free-standing lattice towers, or of slender structures such as cables and transmission lines, if the size of the individual structural members is small relative to the oncoming-flow eddy dimensions, the flow around them can be assumed quasi-steady and locally uniform. This allows the use of steady-flow aerodynamic characteristics to predict the behavior of these line-like structures in the along wind direction, as suggested by Davenport (17), Vickery (79) and Etkin (20). The adequacy of the various assumptions of the method has been examined more recently by Vickery and Kao (80), Bearman (9, 10) and Hunt (39, 40). Obviously, for large bluff bodies (dimensions of the order of the characteristic eddy sizes in the oncoming flow) such an approach is inapplicable. Actually, the relationship between the fluctuating pressures on the body and the fluctuations in the approaching velocity field (in particular, gusts which do not envelop the structure) is not well understood. Related problems are the effects of free stream turbulence on the near wake structure and on vortex shedding; and the distortion effect of the body on the turbulence structure approaching it, all of which should depend on the scale as well as on the intensity of the turbulence.

A theory of turbulent flow around two-dimensional bluff bodies, in which a calculation method for the turbulent velocity outside and upstream of the regions of separated flow is developed under certain conditions on Reynolds number and on the intensity and length scale of the upstream turbulence, has been put forward by Hunt (39, 40). Essentially, the theory ignores wake and boundary layer effects, assuming that the turbulent velocity fluctuations in the wake, in the boundary layers, and in the external flow are statistically independent. The analysis yields the fluctuating velocities and pressures (spectra and correlations) in the

external region, due to the presence of the body, in terms of the properties of the upstream turbulence. The results (which apply to the upstream face of a body, particularly in the area around stagnation) show that the modification of the incident turbulence by the body occurs in two ways: i) through vortex stretching caused by the mean flow field about the body (the major effect as $L_x^u/d \to 0$), and ii) by a simple blocking of the flow by the body (the predominant effect as $L_x^u/d \to \infty$). A combination of these effects was observed by Bearman (9, 10) in experiments with a flat plate for $L_x^u/d \sim 1$ $(1.2 < L_x^u/d < 2.4)$, the axial turbulent velocity component showing attenuation of energy at low wave numbers and amplification at high wave numbers. Space limitations preclude further discussion of these and other theoretical and related experimental results (64, 65, 66). In particular, Sadeh and Bauer (64) have recently provided elaborate visual evidence of vortex stretching and vorticity amplification in stagnation flow round a circular cylinder. Further experimental work seems to be needed, however, especially in regard to nonlinear effects and the (nonstagnation) effects of incident turbulence on boundary layers and wake.

Experimental studies of the effects of incident turbulence have encountered Reynolds number and turbulence length-scale limitations. In most wind tunnels, with appropriate grids used to produce the desired free stream turbulence, to obtain $L_x^u > d$ the cylinder diameter must be sufficiently small, and this implies relatively low Re. The fact that with sufficiently large surface roughness one can obtain supercritical flow at relatively low Re has not yet been fully exploited to explore experimentally the supercritical regime.

The measurements of Surry (72) at subcritical Re (about 4×10^4) were carried out in homogeneous grid-turbulence fields with longitudinal intensities greater than 10% and longitudinal correlation scales ranging from 0.36 d to 4.40 d (see Table 1). Two-point pressure correlations were measured at sufficient number of points (157 angle pairs were examined for each lateral spacing) and then integrated to obtain the statistical properties of the fluctuating lift and drag. The mean pressure distributions on the cylinder disclosed appreciable effects of both intensity and length scale of the turbulence. Surry found that his results could be logically ordered in terms of Taylor's parameter, $T = (u/U)/(D/L_y^u)^{1/5}$,

in agreement with the idea that free stream turbulence tends to promote boundary-layer characteristics associated with higher Re. As T increased from 0.015 (empty tunnel) to 0.161 ($L_x^u/d = 0.36$), S was found to increase from 0.19 to 0.22 and C_d to decrease from 1.31 to 0.93, the mean pressure distributions changing consistently toward those associated with higher Re. However, the parameter T was originally derived with some crude approximations and its application to bluff body flows requires additional clarification. Actually, in a somewhat simplified manner, the effect of free stream turbulence on the flow round a bluff body can be thought of as having two aspects: the interaction between free stream turbulence and the separated shear layers and the near wake on the one hand, and the direct effect on the flow in the cylinder boundary layers, which may lead to changes in the position of transition and separation, on the other (these two mechanisms in general would be coupled). The boundary-layer interaction effect leads to the concept of an effective Re, and it is in this sense that the parameter T , which Bearman (12) has correlated with the critical Re at which the flow changes from subcritical to critical, can help organize the experimental data. It is not likely, however, that this parameter can describe entirely the effect of the approach turbulence, nor is it likely that the changes described in this and the following paragraphs can be explained just by adducing a change in effective Re. In fact, large-scale incident turbulence could affect drastically the shear-layer and near wake flow, and thus the shedding process.

It is interesting to note in this connection that in the case of cooling-tower flows with large surface roughness a comparison of model and prototype data (26, 28) appears to indicate very small, if any, free-stream turbulence effects on certain mean pressure distribution parameters, in particular on the parameter $C_{pb} - C_{pm}$ discussed earlier in this review.

Surry's pressure fluctuating spectra showed that the primary effect of the large-scale turbulence inputs on the shedding was to broaden and lower somewhat the spectral peaks (which were present in all cases). For the small scale input only the lowering was present (and the shift in S). The measurements of Bruun and Davies (16) (see below), on the other hand, did not disclose any changes in the spectral peaks for $T_u = 3.8\%$ ($Re = 0.8 \times 10^5$) and $T_u = 0.16\%$ ($Re = 2.4 \times 10^5$, different).

The C'_p distributions measured by Surry are fairly different for different turbulence inputs, the values in the frontal area around stagnation being dominated by the incident turbulence (8, 10, 72) in agreement with the theoretical predictions discussed earlier. For $L^u_x/d = 0.36$ ($T = 0.161$) C'_p in the wake region dropped to values smaller than for the empty tunnel, the maximum $C'_p \sim 0.4$ being approximately the same but occurring much further downstream; this behavior is consistent with the idea of a higher effective Re for this flow. The C'_p distributions for the larger-scale inputs are more "uniform": for $u/U = 14.7\%$, $C'_p = 0.3$ at stagnation, $= 0.45$ at the peak, and $= 0.35$ at $\theta = 180^\circ$.

Root-mean-square lift and drag coefficients were obtained by Surry for the turbulence input with the largest scale and intensity. Comparison of these results with Sonneville's (71) results in a smooth stream shows that while the fluctuating drag force is much larger in the turbulent stream ($C'_d \sim 0.125$ in Sonneville's measurements, $C'_d \sim 0.26$ in Surry's) the lift is hardly changed by the turbulence, Surry's value being $C'_L \sim 0.53$ (the smooth stream measurements reviewed earlier give C'_L values between 0.45 and 0.50). The qualities of the input turbulence appear to dominate the drag response, without significantly changing C'_L, although there may be changes in the lift spectral distribution (see also below). The domination of the lift response by the shedding is depicted further by the lift cross spectra (peak band widths are fairly broad, however); the drag cross spectra diminish rapidly with increasing lateral spacing and frequency, and the peak at $2 f_s$ appears to be buried by the turbulence response.

Narrow-band lateral pressure correlations measured by Surry to isolate the effect of the incident turbulence on the shedding showed a definite reduction in the case of the large-scale inputs ($L^u_x/d \sim 4$) but very little change for the small-scale incident turbulence, compared with the empty tunnel results. This again indicates that the prime interaction at this small scale ($L^u_x/d \sim 0.4$) is with the boundary layer, as suggested earlier by the pressure fluctuations spectra and C'_p values, and not directly with the separated shear layers and the wake. Typical lateral length scales obtained from the narrow band correlations were of the order of 6 diameters for the small-scale incident turbulence and 4 to 5 diameters for the large-scale inputs, between angles θ of 30 to 150 degrees.

In the light of these results it is clear that the action of incident turbulence cannot be considered simply as equivalent to an increase in Re, particularly for large-scale turbulence. Additional investigations are needed at subcritical Re, continuing the work of Surry, for detailed comparison with Sonneville's (71) results.

Bruun and Davies' (16) results for the 3.8% turbulence intensity stream (see Table 1) were subcritical, with $Re = 8 \times 10^4$ and $C_d = 1.12$. The level of the low frequency part of the pressure spectra for $\theta < 90^\circ$ was found to be higher than the corresponding level of their subcritical smooth stream results ($Re = 2.4 \times 10^5$), the largest increase occurring around stagnation. At $\theta = 0$, a small vortex shedding peak could be seen. (Surry's results show that this peak disappears with increasing turbulence intensity.) Furthermore, the level of the low-frequency part of the pressure spectrum at $\theta = 0$ was higher than the level of the corresponding turbulent velocity spectrum, due to the vortex-shedding contribution. Re-evaluation of Surry's data confirmed this result, which puts a question mark on the assumption of independence of the pressure fluctuations in the frontal part of a bluff body from vortex shedding and wake processes as used in the theoretical analyses described earlier. Sonneville's (71) findings about the role of the low frequency modulations of the shedding process support these conclusions, and suggest as well a direct interaction of the incident turbulence with the shedding in view of the noted increase in the spectra at low frequencies. In general Bruun and Davies' subcritical results confirm Surry's, although there is no complete quantitative agreement, which may be due to the differences in Re. The decrease in the broad band correlation lengths due to the incident turbulence and its effect on the boundary layer flow and on the shedding process and near wake, was also observed. The maximum C'_p was about 0.50, descresing to about 0.35 in the wake.

In the critical Re range the incident turbulence appears to affect the pressure fluctuation levels on the whole of the cylinder (8, 16). The effect is comparatively less on the rear of the cylinder, but C'_p still changes by a factor of 2 in the wake region according to (16) for incident turbulence of about 10% intensity (see Table 1; comparison in (16) is with a flow with $T_u = 0.17\%$, at $Re = 4.8 \times 10^5$, critical). On the

area around stagnation, on the other hand, C'_p is nearly linearly dependent on T_u. No vortex shedding was detected by Bruun and Davies (16) for the three critical flow cases investigated (T_u = 10%) and their results are generally similar to those of Batham's (8) critical flows. The axial pressure-correlation lengths are much shorter than when vortex shedding is present, between about 0.2 d and 0.7 d for all angles θ, and are closely related in the frontal part of the cylinder to the correlation lengths of the incident turbulence (8, 16). Measurements of the pressure fluctuations at the stagnation point by Bearman (9, 10) (the model was a flat plate with a potential flow afterbody) have shown that at low wave numbers the level of the pressure fluctuations can be predicted by applying Bernoulli's equation. For $L^u_x >> d$, the validity of linearizing Bernoulli's equation for calculation of the stagnation pressures (a method that gives C'_p ($\theta = 0$) = 2 T_u for $L^u_x/d \to \infty$, see (10)) has been examined by Bearman (10), Hunt (39), and Bruun and Davies (16), with negative results other than the one just mentioned for low wave numbers. A plot of C'_p ($\theta = 0$)/2 T_u versus L^u_x/d (16) shows ordinate values of about 0.80 for $L^u_x/d = 2$. More importantly, the measured pressure spectra fall off below the velocity spectra rather than showing an increase as predicted by the analysis. The more realistic calculations of Hunt (39, 40) give better agreement (16) with the measured spectra.

Batham (8) carried out pressure fluctuation measurements on a smooth and a rough cylinder, at $Re_1 = 1.1 \times 10^5$ and $Re_2 = 2.4 \times 10^5$, in grid turbulence with $L^u_x/d = 0.5$, $L^u_y/d = 0.2$, and $T_u = 12.9\%$. For the smooth model the spectra exhibit no peaks; the C'_p distributions in the frontal area of the cylinder again appear to be dominated by the incident turbulence and are in general agreement with Bruun and Davies' (16) results. Some evidence that at Re_1 the fluctuations in the wake influence the overall pressure distribution is provided by the circumferential pressure correlations measured by Batham. Also, at Re_1, $C'_L = 0.14$ is higher than $C'_L = 0.09$ at Re_2, but both are typical critical regime values.

Batham's measurements with the rough model are important in that, at Re_2, they appear to be the only available measurements of the effect of incident turbulence on a cylinder in the supercritical regime. At Re_2 the spectra show well-defined peaks, as did the spectra for the rough

cylinder in the smooth stream at the same Re. Furthermore, the C'_p distribution is similar to that observed on a rough cylinder in turbulent flow at $Re = 7.1 \times 10^5$ (unpublished results of Tunstall cited by Batham) and exhibits a second C'_p peak at $\theta = 150^\circ$, probably associated with a high frequency energy content at this angle.

The spectral peaks at Re_2 do not seem significantly affected by the incident turbulence; they actually seem somewhat larger for the turbulent stream, possibly due to earlier transition in the boundary layer resulting in a wider wake. (The smooth-stream rough-cylinder flow at Re_2 is probably at the beginning of the supercritical range.) Complete-signal pressure correlation lengths around the front of the cylinder were smaller due to the incident turbulence, which had relatively small scales. At Re_2, the higher level of coherent shedding gave rise to larger correlation lengths from $\theta = 60^\circ$ to $\theta = 150^\circ$, about 2.5 d. Narrow-band correlations were not obtained by Batham. The rough-cylinder turbulent-stream C'_p levels at Re_2 for $\theta > 60^\circ$ are larger than the corresponding levels at Re_1, due to the presence of coherent shedding, and $C'_L = 0.27$ at Re_2, as opposed to $C'_L = 0.15$ at Re_1. The C'_D levels are not much different for the two Reynolds numbers: 0.086 at Re_2, 0.072 at Re_1. The difference could be due to low frequency modulations of the shedding as described by Sonneville for subcritical flow.

It should be noted that C'_p at Re_2 is much larger in the rough-turbulent than in the rough-uniform case, in agreement with the higher level of coherent shedding; also, $C'_L = 0.15$ in the rough-uniform case, smaller than $C'_L = 0.27$ cited above.

CONCLUSIONS

While the dependence of the mean pressures on circular cylindrical structures in uniform flow, on both Reynolds number and surface roughness, has been the object of several recent investigations, corresponding studies for parameters characterizing the fluctuating loads (Strouhal number, r.m.s. lift, drag and pressure coefficients, correlations and spectra of the fluctuations) are in general still needed, in particular for critical, supercritical and transcritical Re. The definition of the various flow regimes and the manner of transition between regimes, both subcritical-critical and critical-supercritical, require further investigation. In particular, a Strouhal band width criterion to characterize spectral peaks is probably needed for a sharp definition of the boundary between the critical and supercritical regimes. Of special interest in connection with the characterization of flow regimes and transitions are three-dimensional effects on the flow and the influence of the inherent flow unsteadiness. A secondary but nonetheless important need is that of a universal terminology for this "new" research topic.

Cross correlation measurements at large Re and/or with large roughness are needed to resolve existing discrepancies and to map fully the characteristics of the flow and the unsteady loading at supercritical Re , as has already been done to a certain extent for subcritical flows. But experimental discrepancies still exist even for subcritical flow, and these require elucidation.

Relatively few studies are presently available regarding free stream turbulence effects on the flow around large circular structures. In the transcritical Re range, with transition occurring very close to the forward stagnation line, further (small) changes in its position by the incident turbulence would not affect the boundary layer flow. But the direct effect of incident turbulence fields (of different scales and intensities) on the pressure fluctuations on the body, and the indirect effect through possible modification of the flow in the turbulent boundary layers and in the separated shear layers and the near wake (and thus on the shedding process) require additional investigation, including the influence of surface roughness of the distributed, longitudinal-rib, or trip-wire type.

ACKNOWLEDGEMENTS

Partial support from National Science Foundation under Grant ENG78-22092 is gratefully acknowledged. This work was completed by the author during a Visiting Professorship at the Universidade Federal do Rio Grande do Sul, in the Laboratório de Aerodinamica das Construcões, Curso de Pós-Graduacão em Engenharia Civil.

REFERENCES

1. Achenbach, E., "The Effect of Surface Roughness on Heat Transfer from a Circular Cylinder to the Cross Flow of Air," Int. Jrnl. Heat Mass Transfer, Vol. 20, 1977, pp. 359-369.

2. Achenbach, E., "Total and Local Heat Transfer from a Smooth Circular Cylinder in Cross Flow at High Reynolds Number," Int. Jrnl. Heat Mass Transfer, Vol. 18, 1975, pp. 1387-1396.

3. Achenbach, E., "Influence of Surface Roughness on the Cross Flow Around a Circular Cylinder," JFM, Vol. 46, 1971, pp. 321-335.

4. Achenbach, E., "Distribution of Local Pressure and Skin Friction Around a Circular Cylinder in Cross Flow up to Re = 5×10^6," JFM, Vol. 34, 1968, pp. 625-639.

5. Abu-Sitta, S.H. and Davenport, A.G., "Design Criteria for Cooling Towers Against Wind," ASCE National Meeting, Session 39, Cincinnati, Ohio, 1974.

6. Abu-Sitta, S.H. and Hashish, M.G., "Dynamic Wind Stress in Hyperbolic Cooling Towers," Jrnl. Structural Division, ASCE, Vol. 99, No. ST9, 1973, pp. 1823-1835.

7. Barnett, K. M., and Cermak, J. E., "Turbulence-Induced Changes in Vortex Shedding from a Circular Cylinder," CSU Fluid Dynamics and Diffusion Laboratory Report, CER 73-74 KMB - JEC27, 1974.

8. Batham, J. P., Pressure Distributions on Circular Cylinders at Critical Reynolds Numbers," JFM, Vol. 57, 1973, pp. 209-228.

9. Bearman, P. W., "Turbulence-Induced Vibrations of Bluff Bodies," Proc. IUTAM-IAHR Symposium on Flow-Induced Structural Vibrations, Karlsruhe, Springer-Verlag, pp. 701-716.

10. Bearman, P. W., "Some Measurements of the Distortion of Turbulence Approaching a Two-Dimensional Bluff Body," JFM, Vol. 53, 1972, pp. 451-467.

11. Bearman, P. W., "On Vortex Shedding from a Circular Cylinder in the Critical Reynolds Number Regime," JFM, Vol. 37, 1969, pp. 577-585.

12. Bearman, P. W., "The Flow Around a Circular Cylinder in the Critical Reynolds Number Region," National Physical Laboratory NPL Aero Report No. 1257, 1968.

13. Bishop, R. E. and Hassan, A. Y., "The Lift and Drag Forces on a Circular Cylinder in a Flowing Fluid," Proc. Roy. Soc. London, Ser. A, Vol. 277, 1964, pp. 32-50.

14. Blevins, R. D., Flow-Induced Vibration, Van Nostrand-Reinhold Co., New York, 1977.

15. Bloor, M. S., "The Transition to Turbulence in the Wake of a Circular Cylinder," JFM, Vol. 19, 1964, pp. 290-302.

16. Bruun, H. H. and Davies, P. O. A. L., "An Experimental Investigation of the Unsteady Pressure Forces on a Circular Cylinder in a Turbulent Cross Flow," Jrnl. Sound and Vibration, Vol. 40(4), 1975, pp. 535-559.

17. Davenport, A. G., "The Application of Statistical Concepts to the Wind Loading of Structures," Proc. Inst. Civil Engineers, Vol. 19, 1961, pp. 449-472.

18. Davenport, A. G. and Isyumov, N., "The Dynamic and Static Action of Wind on Hyperbolic Cooling Towers," Univ. Western Ontario, Canada, Engineering Sciences Research Rep. BLWT-1-66, 1966.

19. El-Sherbiny, Saad El-Sayed, "Effects of Wall Confinements on the Aerodynamics of Bluff Bodies," Ph.D. Thesis, Dept. of Mech. Engineering, Univ. British Columbia, Vancouver, Canada, 1972.

20. Etkin, B., "Theory of the Response of a Slender Cylindrical Structure to a Turbulent Wind with Shear," Meeting on Ground Wind-Load Problems, NASA, Langley, 1966.

21. Etkin, B., Korbacher, G., and Keefe, R., Jrnl. Acoustical Society of America, Vol. 29, 1957, p. 30.

22. Ezra, A. A. and Birnbaum, S., "Design Criteria for Space Vehicles to Resist Wind-Induced Oscillation," ARS Journal, 1961.

23. Fage, A. and Falkner, V. M., "Further Experiments on the Flow Around a Circular Cylinder," ARC R&M, No. 1369, 1931.

24. Fage, A. and Warsap, J. H., "The Effects of Turbulence and Surface Roughness on the Drag of a Circular Cylinder," ARC R&M 1283, 1929.

25. Farell, C., Carrasquel, S., Güven, O., and Patel, V. C., "Effects of Wind Tunnel Walls on the Flow Past Circular Cylinders and Cooling Tower Models," Jrnl. Fluids Engineering, Trans. ASME, Vol. 99, Series I, No. 3, 1977, pp. 470-479.

26. Farell, C., Güven, O., and Maisch, F., "Mean Wind Loading on Rough-Walled Cooling Towers," Jrnl. Engineering Mechanics Division, ASCE, Vol. 102, No. EM6, 1976, pp. 1059-1081.

27. Farell, C., Güven, O., and Patel, V. C., "Laboratory Simulation of Wind Loading of Rounded Structures," Proc. IASS World Congress on Space Enclosures, Montreal, 1976.

28. Farell, C. and Patel, V. C., "Flow Around Rounded-Walled Structures; Experimental and Analytical Studies," 1977 ASCE Annual Convention, San Francisco, California.

29. Ffowcs Williams, J. E. and Hawkings, D. L., "Sound Generation by Turbulence and Surfaces in Arbitrary Motion," Phil. Trans. Roy. Soc., Series A, Vol. 264, 1969, p. 321.

30. Fung, Y. C., "Fluctuating Lift and Drag Acting on a Cylinder in a Flow at Supercritical Reynolds Number," Jrnl. Aerospace Science, Vol. 27, 1960.

31. Gerrard, J. H., "The Three-Dimensional Structure of the Wake of a Circular Cylinder," JFM, Vol. 25, 1966, pp. 143-164.

32. Gerrard, J. H., "A Disturbance-Sensitive Reynolds Number Range of the Flow Past a Circular Cylinder," JFM, Vol. 22, 1965, pp. 197-196.

33. Goldman, R. L., "Karman Vortex Forces on Vanguard Rocket," Shock and Vibration Bulletin, Part II, Naval Research Laboratory, Washington, D.C., 1958.

34. Güven, O., Farell, C., and Patel, V. C., "Surface Roughness Effects on the Mean Flow Past Circular Cylinders," to be published in JFM, 1979.

35. Güven, O., Patel, V. C., and Farell, C., "A Model for High Reynolds Number Flow Past Rough-Walled Circular Cylinders," Jrnl. Fluids Engineering, Trans. ASME, Vol. 99, Series I, No. 3, 1977, pp. 486-494.

36. Hashish, M. G. and Abu-Sitta, S. H., "Response of Hyperbolic Cooling Towers to Turbulent Wind," Jrnl. Structural Division, ASCE, Vol. 100, No. ST5, Proc. Paper 10542, 1974, pp. 1037-1051.

37. Humphreys, J. S., "On a Circular Cylinder in Steady Wind at Transition Reynolds Numbers," JFM, Vol. 9, 1960, pp. 603-612.

38. Humphreys, J. S., "On a Circular Cylinder in a Steady Wind," Ph.D. Thesis, Harvard University, 1959.

39. Hunt, J. C. R., "A Theory of Turbulent Flow Round Two-Dimensional Bluff Bodies," JFM, Vol. 61, Pt. 4, 1973, pp. 625-706.

40. Hunt, J. C. R., "A Theory for Fluctuating Pressures on Bluff Bodies in Turbulent Flows," Proc. IUTAM-IAHR Symposium on Flow-Induced Structural Vibrations, Karlsruhe, Germany, Springer-Verlag, 1972, pp. 190-203.

41. Jones, G. W., Cincotta, J. J., and Walker, R. W., "Aerodynamic Forces on a Stationary and Oscillating Circular Cylinder at High Reynolds Numbers," NASA Technical Rep., NASA TR R-300, 1969.

42. Keefe, R. T., "An Investigation of the Fluctuating Forces Acting on a Stationary Circular Cylinder in a Subsonic Stream and of the Associated Sound Field," Univ. Toronto, Inst. Aerophys, Rep. No. 76, 1961.

43. Kestin, J. and Wood, R. T., "On the Stability of Two-Dimensional Stagnation Flow," Jrnl. Fluid Mechanics, Vol. 44, Part 3, 1970, pp. 461-479.

44. Korotkin, A. I., "The Three-Dimensionality of the Flow Transverse to a Circular Cylinder," Fluid Mechanics - Soviet Research, Vol. 5, No. 2, 1976.

45. Lee, B. E., "Some Effects of Turbulence Scale on the Mean Forces on a Bluff Body," Jrnl. Industrial Aerodynamics, Vol. 1, 1975, pp. 361-370.

46. Lee, G. E., "The Effects of Turbulence on the Surface Pressure Field of a Square Prism," JFM, Vol. 69, 1975, pp. 263-282.

47. Lienhard, J. H., "Synopsis of Lift, Drag, and Vortex Frequency Data for Rigid Circular Cylinders," Washington State University, College of Engineering Research Division Bulletin No. 300, 1966.

48. Macovsky, M., "Vortex Induced Vibration Studies," U.S. Navy Dept., David Taylor Model Basin Rep. 1190, 1968.

49. Marris, A. W., "A Review on Vortex Streets, Periodic Wakes, and Induced Vibration Phenomena," Jrnl. Basic Engineering, Trans. ASME, Ser. D, Vol. 86, pp. 185-196.

50. Mattingly, G. E., "An Experimental Study of the Three-Dimensionality of the Flow Around a Circular Cylinder," Institute for Fluid Dynamics and Applied Mathematics, Univ. of Maryland Tech. Note BN-295, 1962.

51. McGregor, D. M., "An Experimental Investigation of the Oscillating Pressures on a Circular Cylinder in a Fluid Stream," Univ. of Toronto Inst. Aerophys. Tech. Note, No. 14, 1957.

52. Morkovin, M. V., "Flow Around a Circular Cylinder - A Kaleidoscope of Challenging Fluid Phenomena," Proc. ASME Symposium on Fully Separated Flows, Philadelphia, Pa., 1964, pp. 102-118.

53. Mulcahy, T. M. and Chen, S. S., "Annotated Bibliography on Flow-Induced Vibrations," Argonne National Laboratory Technical Memorandum ANL-CT-74-05, 1974.

54. Nakamura, Y., "Some Research on Aeroelastic Instabilities of Bluff Structural Sections," Research Institute for Applied Mechanics, Kyushu University, Japan, 1975.

55. Naumann, A. and Quadflieg, H., "Vortex Generation on Cylindrical Buildings and Its Simulation in Wind Tunnels," Proc. IUTAM-IAHR Symposium on Flow-Induced Structural Vibrations, Karlsruhe, Germany, Springer-Verlag, 1972, pp. 730-747.

56. Naumann, A. and Quadflieg, H., "Aerodynamic Aspects of Wind Effects on Cylindrical Buildings," Proc. Symp. Wind Effects on Buildings and Structures, Vol. 1, Loughborough, England, 1968.

57. Niemann, H. J., "On the Stationary Wind Loading on Axisymmetric Structures in the Transcritical Reynolds Number Region," Institute fur Konstruktiven Ingenieurbau Rep. No. 71-2, Ruhr-Univ. Bochum., 1971.

58. Van Nunen, J. W. G., Persoon, A. J. , and Tijdeman, "Analysis of Steady and Unsteady Measurements on a Circular Cylinder in a Cross Flow at Reynolds Numbers up to 7.7×10^6," Proc. IUTAM/IAHR Symposium on Flow-Induced Structural Vibrations, Springer-Verlag, p. 748; also National Aerospace Lab. Rep. NLR TR 69102 U, The Netherlands (1971), 1972.

59. Propper, H., "Zur Aerodynamischen Belastung Grosser Kühltürme," Institut für Konstructiven Ingenierbau Rep. No. 77-3, Ruhr-Univ. Bochum, 1977.

60. Richter, A. and Naudascher, E., "Fluctuating Forces on a Rigid Circular Cylinder in Confined Flow," JFM, Vol. 78, 1976, pp. 561-576.

61. Roshko, A., "Experiments on the Flow Past a Circular Cylinder at Very High Reynolds Number," JFM, Vol. 78, 1961, pp. 561-576.

62. Roshko, A., "On the Development of Turbulent Wakes from Vortex Streets," NACA Rep. 1191, 1954, pp. 19.1-19.17.

63. Roshko, A. and Fiszdon, W., "On the Persistence of Transition in the Near Wake," Problems of Aerodynamics and Continuum Mechanics, Society for Industrial and Applied Mathematics, Philadelphia, Pa., 1969, pp. 606-616.

64. Sadeh, W. Z. and Brauer, H. J., "A Visual Investigation of Turbulence in Stagnation Flow About a Circular Cylinder," NASA Contractor Report 3019, Colorado State University, 1978.

65. Sadeh, W. Z. and Cermak, J. E., "Turbulence Effect on Wall Pressure Fluctuations," Jrnl. Engineering Mechanics Division, ASCE, Vol. 98, No. EM6, 1972, pp. 1365-1379.

66. Sadeh, W. Z., Sutera, S. P., and Maeder, P. F., "An Investigation of Velocity Amplification in Stagnation Flow," ZAMM, Vol. 21, 1970, pp. 717-742.

67. Savkar, S. D., "A Survey of Flow-Induced Vibrations of Cylindrical Arrays in Cross-Flow," General Electric Company Technical Information Series Report 76 CRD 139, 1976.

68. Savkar, S. D. and So, R. M. C., "On the Buffeting Response of a Cylinder in a Turbulent Cross Flow," General Electric Report GEAP-24149, 1978.

69. Schmidt, L. V., "Fluctuating Force Measurements Upon a Circular Cylinder at Reynolds Numbers up to 5×10^6," NASA Paper, Meeting on Ground Wind-Load Problems in Relation to Launch Vehicles, NASA Langley Research Center, NASA TMX-57779, 1966, pp. 19.1-19.17.

70. Schmidt, L. V., "Measurements of Fluctuating Air Loads on a Circular Cylinder," Jrnl. Aircraft, Vol. 2, No. 1, 1965, pp. 49-55.

71. Sonneville, P., "Etude de la Structure Tridimensionnelle des Écoulements Autour d'un Cylindre Circulaire," Bulletin Direction des Études et Recherches, Electricité de France, Serie A, No. 3, 1976.

72. Surry, D., "Some Effects of Intense Turbulence on the Aerodynamics of a Circular Cylinder at Subcritical Reynolds Number," JFM, Vol. 52, 1972, pp. 543-563.

73. Szechenyi, E., "Supercritical Reynolds Number Simulation for Two-Dimensional Flow Over Circular Cylinders," JFM, Vol. 70, 1975, pp. 523-542.

74. Szechenyi, E., "Simulation de Nombres de Reynolds Élevés sur un Cylindre en Soufflerie," La Recherche Aérospatiale, 1974, pp. 155-164.

75. Szecheni, E. and Loiseau, H., "Portances Instationnaires sur un Cylindre Vibrant dans un Écoulement Supercritique," La Recherche Aérospatiale, 1975, pp. 45-57.

76. Tani, I., "On the Periodic Shedding of Vortices from a Circular Cylinder at High Reynolds Numbers," Proc. IUTAM Symposium on Concentrated Vortex Motions in Fluids, Ann Arbor, Michigan, 1964.

77. Tani, I., "Critical Survey of Published Theories on the Mechanism of Leading-Edge Stall," Aeronautical Research Institute, Univ. of Tokyo, Rep. No. 367, 1961.

78. Vickery, B. J., "Fluctuating Lift and Drag on a Long Cylinder of Square Cross Section in a Smooth and in a Turbulent Stream," JFM, Vol. 25, 1966, pp. 481-494.

79. Vickery, B. J., "On the Flow Behind a Coarse Grid and Its Use as a Model of Atmospheric Turbulence in Studies Related to Wind Loads on Buildings," NPL Aero Report 1143, 1965.

80. Vickery, B. J. and Kao, K. H., "Drag or Along-Wind Response of Slender Structures," Jrnl. Structural Division, ASCE, Vol. 98, No. STI, 1972, pp. 21-36.

81. Warschauer, K. A. and Leene, J. A., "Experiments on Mean and Fluctuating Pressures on Circular Cylinders at Cross Flow at Very High Reynolds Numbers," Proc. Conference on Wind Effects on Buildings and Structures, Tokyo, 1971, pp. 305-315.